the SILK ROAD PROJECT at NAOC

丝绸之路[a]计划 And ARI/ZAH

ZENTRUM FÜR ASTRONOMIE

ARI ITA LSW Univ. Heidelberg

Past, Present, and Future of Direct N-Body Simulations more than a million stars...

Rainer Spurzem, and Silk Road Team

Astronomisches Rechen-Inst., ZAH, Univ. of Heidelberg, Germany

National Astronomical Observatories (NAOC), Univ. of Chinese Academy of Sciences

Kavli Institute for Astronomy and Astrophysics (KIAA), Peking University

Picture:
Xi Shuang Banna, Yunnan, SW China (R.Sp.)

spurzem@ari.uni-heidelberg.de

http://silkroad.bao.ac.cn

VolkswagenStiftung

Team Members and Collaborators

Albrecht Kamlah, Manuel Arca Sedda, Francesco Rizzuto, Thorsten Naab, Jeremiah Ostriker, Mirek Giersz, Margaryta Sobolenko, Peter Berczik, Qi Shu, Bhusan Kayastha, Agostino Leveque, Arek Hypki, Long Wang, Thijs Kouwenhoven, Marina Ischenko, Nicholas Stone, Bhusan Kayastha, Ricarda Heilemann, Julia Hauer

- Kamlah et al. 2021/2022: Preparing the next gravitational million-body simulations: Evolution of single and binary stars in Nbody6++GPU, MOCCA and McLuster, 2021, Monthly Notices of the Royal Astronomical Society, in press, arxiv:2105.08067
- Arca-Sedda et al. 2021, Breaching the Limit: Formation of GW190521-like and IMBH Mergers in Young Massive Clusters, 2021, The Astrophysical Journal, 920, 128
- Rizzuto et al. 2021:, Intermediate mass black hole formation in compact young massive star clusters, 2021, Monthly Notices of the Royal Astronomical Society, 501, 5257 (Paper I, Paper II 2022 in review).

<u>Today not presented:</u>

- **Stardisk and nuclear star clusters, single and binary supermassive black holes** *(Peter Berczik, Li Shuo, Zhong Shiyan, Kimitake Hayasaki, Andreas Just, Gaia Fabj, Marija Minzburg, Philip Cho)*
- **Planetary Systems in Star Clusters (SPP1992):** Katja Stock, Francesco Flammini, Paul Zürn, Stephanie Gutmayer, Maxwell Cai, Simon Portegies Zwart

CAMK
Warsaw

1) **Introduction – History**
2) Star Cluster Dynamics with Black Holes and Gravitational Waves
1) Star Clusters with IMBH formation
2) Code(s) and Hardware

some history

Astronomisches Rechen-Institut in Heidelberg
Mitteilungen Serie A Nr. 14

Die numerische Integration des n-Körper-Problemes für Sternhaufen I

Von

SEBASTIAN VON HOERNER

Mit 3 Textabbildungen

(Eingegangen am 10. Mai 1960)

Astronomisches Rechen-Institut in Heidelberg
Mitteilungen Serie A Nr. 19

Die numerische Integration des n-Körper-Problems für Sternhaufen, II.

Von

SEBASTIAN VON HOERNER

Mit 10 Textabbildungen

(Eingegangen am 19. November 1962)

Sebastian von Hoerner
(1919 – 2003)

Dynamics of Star Clusters and the Milky Way
ASP Conference Series, Vol. 228, 2001
S. Deiters, B. Fuchs, A. Just, R. Spurzem, and R. Wielen, eds.

How it All Started

Sebastian von Hoerner

Krummenackerstraße 186, 73733 Esslingen, Germany

After having worked for turbulence and shock fronts, I changed 1956 to the structure and dynamics of star clusters, but soon I found this somewhat frustrating. Before starting a theoretical treatment, one had to make so many assumptions and approximations, that I did not know how much of the final results one really could believe. I would have loved to try it a completely different way, by "Experimental Mathematics", so to say. Just make a little cluster of stars, with random locations and random velocities, put it on a computer, integrate Newton's gravity in small time steps, and just look and see what the little thing really does. Without any assumptions or approximations to start with. Well, one assumption: that treating a small number will already make sense.

This would need two new things: random numbers, and a fast computer. The first one did exist: in 1956 I had invented a method to create fairly good random numbers, which stayed in general use for some years. But the second one did not. Our first electronic computer, finished 1952 by the Max-Planck-Institut at Göttingen, G1, made 5 operations/sec (fixed point), and had a memory of 26 numbers. It used 476 vacuum tubes (and 101 relays). And with a lifetime of, say 4 years per tube, this gives every three days a breakdown (of computer and user). Nevertheless, we gladly used it day and night. The next one, the G2 in 1955, hat about ten times the speed and the memory. Good progress; but a square root still took 0.6 seconds. – Integrating a little cluster, of only N = 10 stars, would mean to handle 6 × N = 60 coupled partial differential equations of second order, and that was completely out of question. Also, each small time step would need N(N-1)/2 = 45 square roots, or 27 seconds for just those roots. – Thus, the whole method wound up in my drawer of "great impossible ideas".

Later used: Siemens 2002 at ARI in Heidelberg...

History

Astronomisches Rechen-Institut in Heidelberg
Mitteilungen Serie A Nr. 14

Die numerische Integration des *n*-Körper-Problemes für Sternhaufen I

Von

Sebastian von Hoerner

Mit 3 Textabbildungen

(Eingegangen am 10. Mai 1960)

Tabelle 5. *Zahl der gegenseitigen Umläufe, Häufigkeit des Auftretens und kleinster gegenseitiger Abstand D_m der engsten Paare.* (Alle engsten Paare mit mehr als zwei vollen Umläufen wurden notiert)

Umläufe	Häufigkeit	D_m
2—3	11	0.0102
3—5	9	0.0177
5—10	5	0.0070
10—20	2	0,0141
20—50	1	0.0007
50—100	1	0.0035
100—200	1	0.0039

Astronomisches Rechen-Institut in Heidelberg
Mitteilungen Serie A Nr. 19

Die numerische Integration des *n*-Körper-Problems für Sternhaufen, II.

Von

Sebastian von Hoerner

Mit 10 Textabbildungen

(Eingegangen am 19. November 1962)

S.v. Hoerner,
Z.f.Astroph. 1960, 63

Siemens 2002
N=4,8,12,16 (4 Trx)

N=16,25 (40 Trx)

Astronomisches Rechen-Institut (ARI) at Univ. of Heidelberg, Germany

Siemens 2002 Computer in 1964 At ARI

On the Evolution of Stellar Systems

V. A. Ambartsumian

(George Darwin Lecture, delivered on 1960 May 13)

IN THIS lecture we shall consider some aspects of the problem of the evolution of stellar systems. We shall concentrate chiefly on *galaxies*. However, at the same time we shall treat here some questions connected with star *clusters* as component members of galaxies.

Concepts discussed:

Total Energy of grav. star clusters NOT additive

No thermodynamical equilibrium

Statistical Theory of Gases to be used with care
(large mean free path)

Locally truncated Maxwellian distribution.

Physical and Numerical Methods: Modelling the Dynamics

$$\vec{a}_0 = \sum_j G m_j \frac{\vec{R}_j}{R_j^3} \quad ; \quad \dot{\vec{a}}_0 = \sum_j G m_j \left[\frac{\vec{V}_j}{R_j^3} - \frac{3(\vec{V}_j \cdot \vec{R}_j)\vec{R}_j}{R_j^5} \right]$$

- $N = \infty$

negative specific Heat

gravothermal Collapse

gravothermal Oscillations

- $N = 3$ $(N = 2, \ldots, \approx 100)$

History

Exponential Instability

Chaos and Resonance

Regularisation

- $N = 10^6$ $(N = 10^4, 10^5)$

Post-Kollaps-Evolution

Binaries

Globular Clusters

Physical and Numerical Methods: Modelling the Dynamics

Some methods for studying the evolution of globular clusters (by D.C.Heggie)

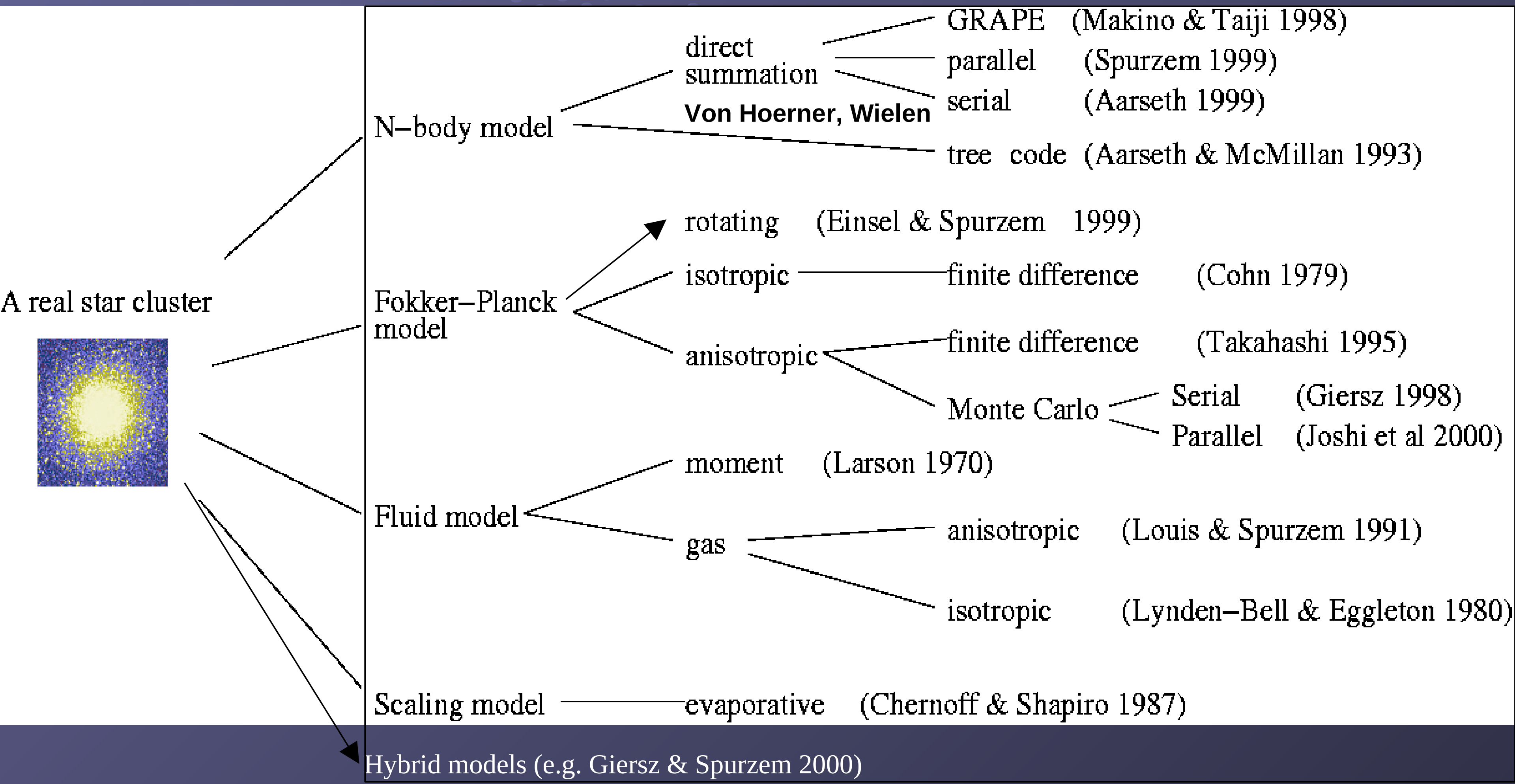

Aarseth, Henon, Wielen, 1974, A&A: A comparison of numerical methods for the study of tar cluster dynamics

N-body Codes:

Von Hoerner
Wielen
Aarseth

independent

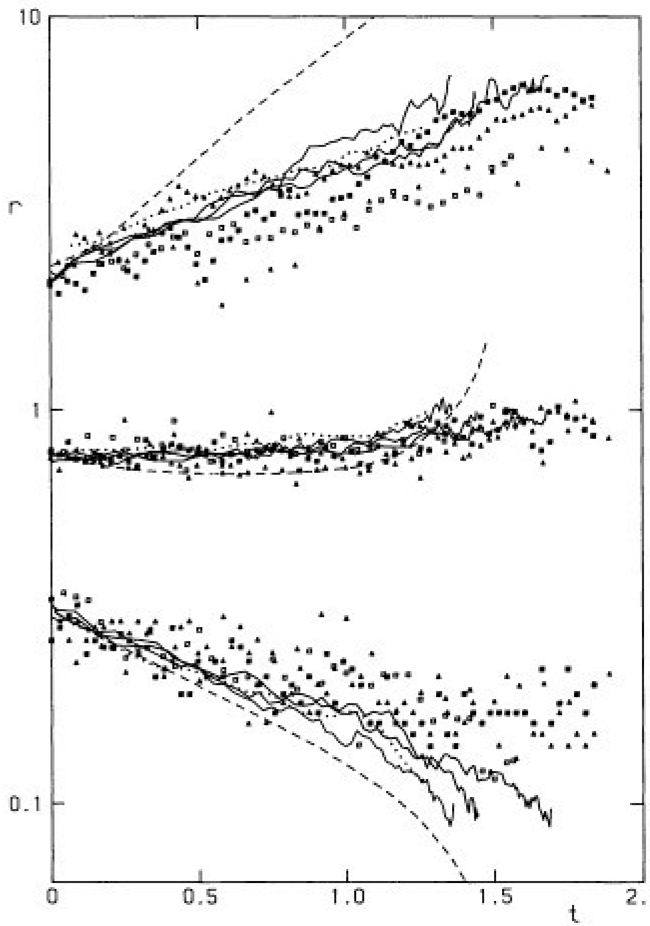

Fig. 1. Radii containing 10%, 50%, 90% of the mass, plotted versus time for a cluster with stars of equal masses. Open triangles and squares: *N*-body integrations with $N=100$ and $N=250$ (Wielen). Filled triangles and squares: *N*-body integrations with $N=250$ (Aarseth). Full lines: Monte Carlo models (Hénon). Dotted lines: Monte Carlo model (Shull and Spitzer). Dashed lines: fluid-dynamical model (Larson)

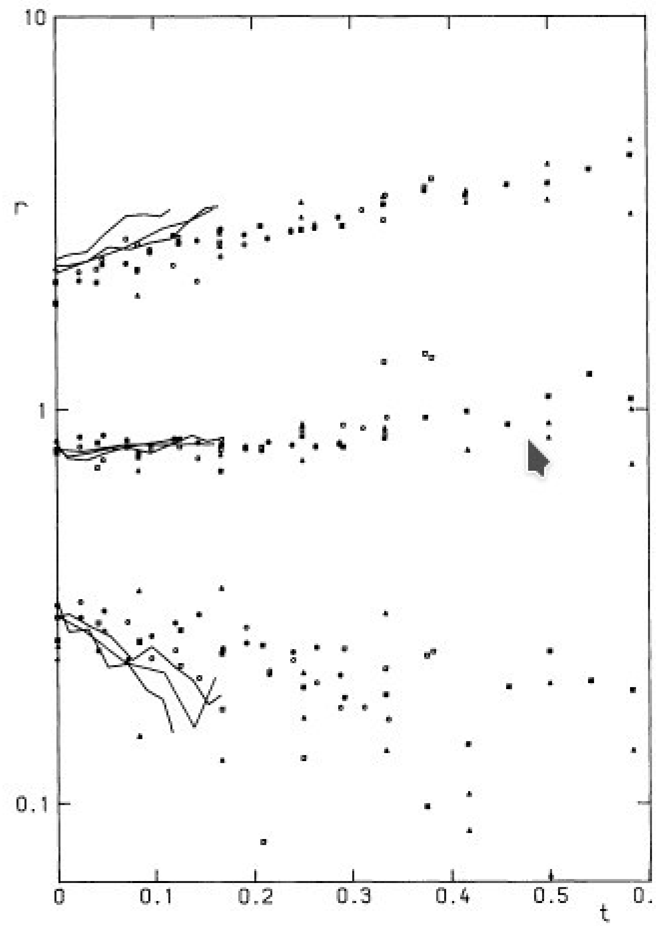

Fig. 2. Radii containing 10%, 50%, 90% of the mass, plotted versus time for a cluster with stars of different masses. Open and filled symbols: *N*-body integrations with $N=100$ (triangles), $N=250$ (squares), $N=500$ (circles) (Wielen). Full lines: Monte Carlo models (Hénon)

Approx. Models I: Gas Sphere

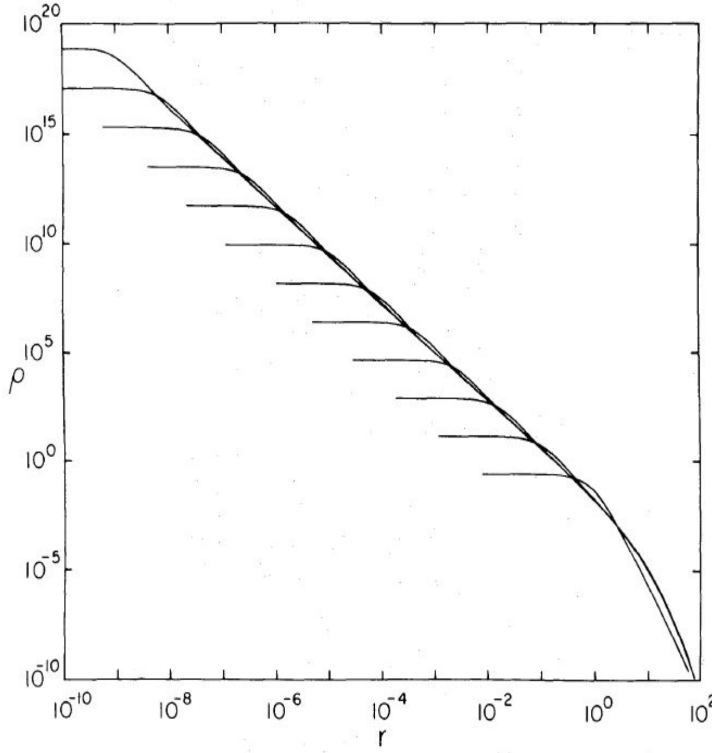

Cohn (1980): Direct Fokker-Planckj model

Core Collapse

Gravothermal Catastrophe

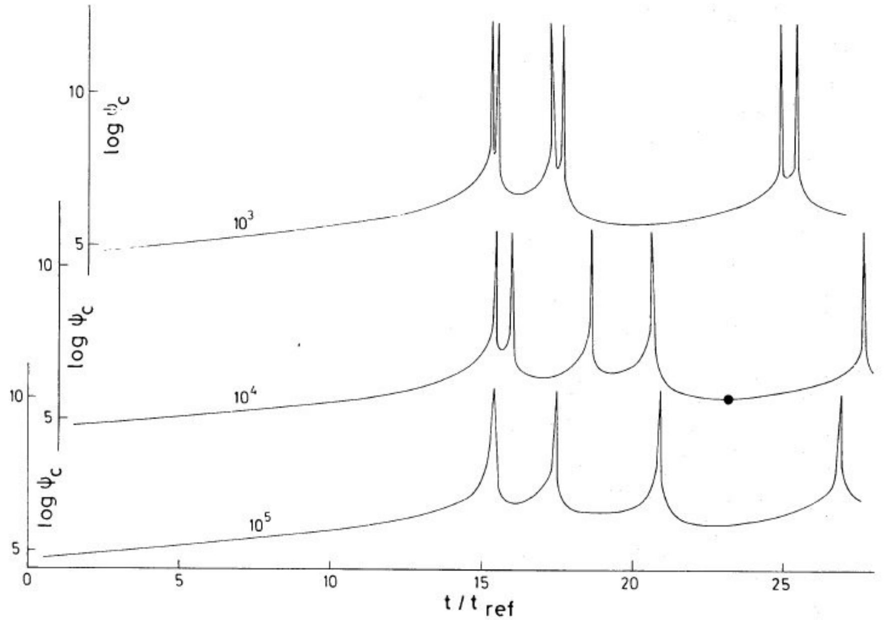

Figure 1. The 'central' density ψ_c is plotted against the non-dimensional time t/t_{ref} for $k = 2$ models with three different values of C as attached to each curve. Note, that if they were plotted with the same ordinate they would be close to each other despite the great differences in C. The model indicated with a filled circle will be compared with King's model in Section 4.2.

Bettwieser & Sugimoto 1984:

Gravothermal Oscillations by

energy generation from binaries

(cf. nuclear stellar energy generation)

3-body Encounters Starlab Simulation (S.L.W. McMillan)

http://www.physics.drexel.edu/~steve/

-> Three-Body-Problem

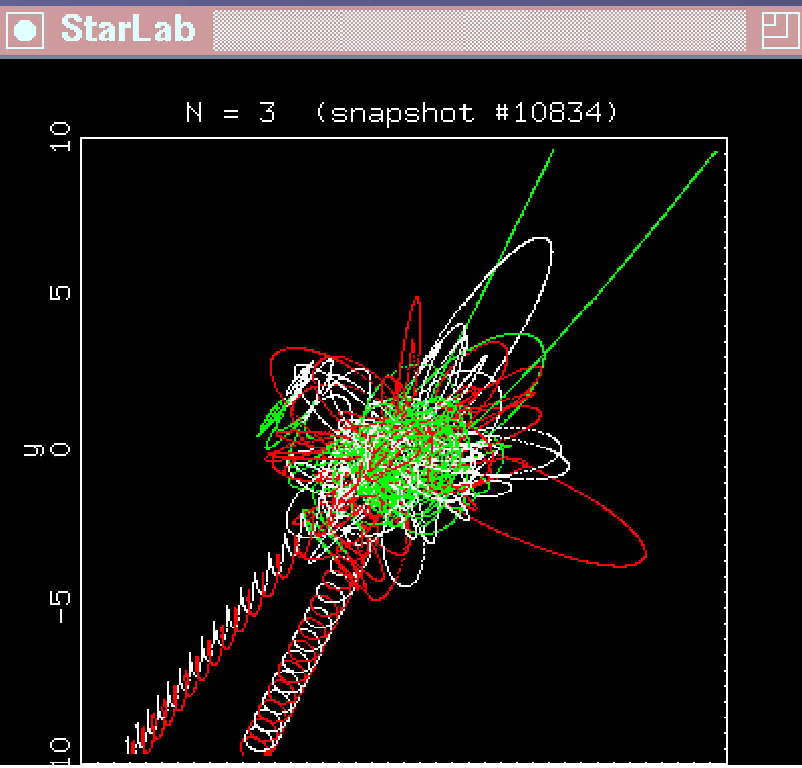

Gravothermal Oscillations - Attractor in Phase Space
Spurzem 1994, Giersz & Spurzem 1994
Amaro-Seoane, Freitag & Sp. 2004

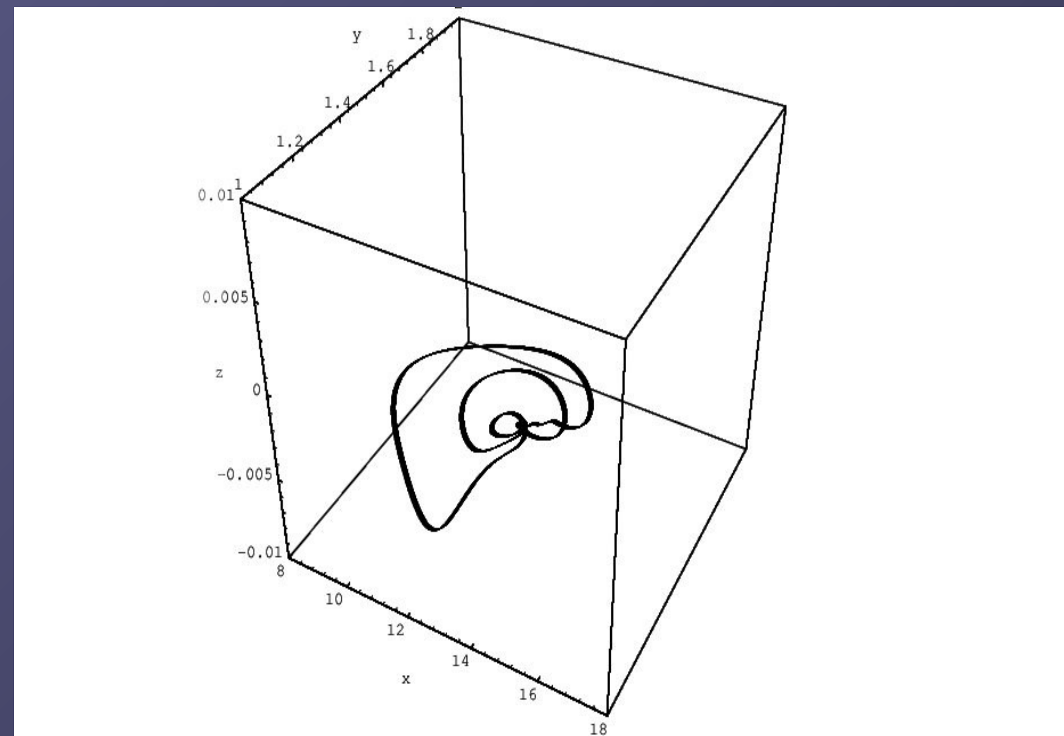

Fig. 3:
-dimensional attractor for $N = 100.000$ system, $x =$ σ'_c, $z = \xi$.

Mon. Not. R. astr. Soc. (1991) **252**, 177–189

Gravothermal instability of anisotropic self-gravitating gas spheres: singular equilibrium solution

R. Spurzem[1,2,3]
[1] *Institut für Theoretische Physik und Sternwarte, University of Kiel, Olshausenstraße 40, D-2300 Kiel, Germany*
[2] *Institut für Astronomie und Astrophysik, University of Würzburg, Am Hubland, D-8700 Würzburg, Germany*
[3] *Universitätssternwarte Göttingen, Geismarlandstraße 11, D-3400 Göttingen, Germany*

Follow-Up of Angeletti & Giannone and Larson

Star2000 Conference Heidelberg: Dynamics of Star Clusters and the Milky Way, ASP Conference Series, Vol. 228.
Edited by S. Deiters, B. Fuchs, R. Spurzem, A. Just, and R. Wielen.
San Francisco: Astronomical Society of the Pacific.

Fokker-Planck N-Body Comparison

Dissolution of Star Cluster in Tidal Field

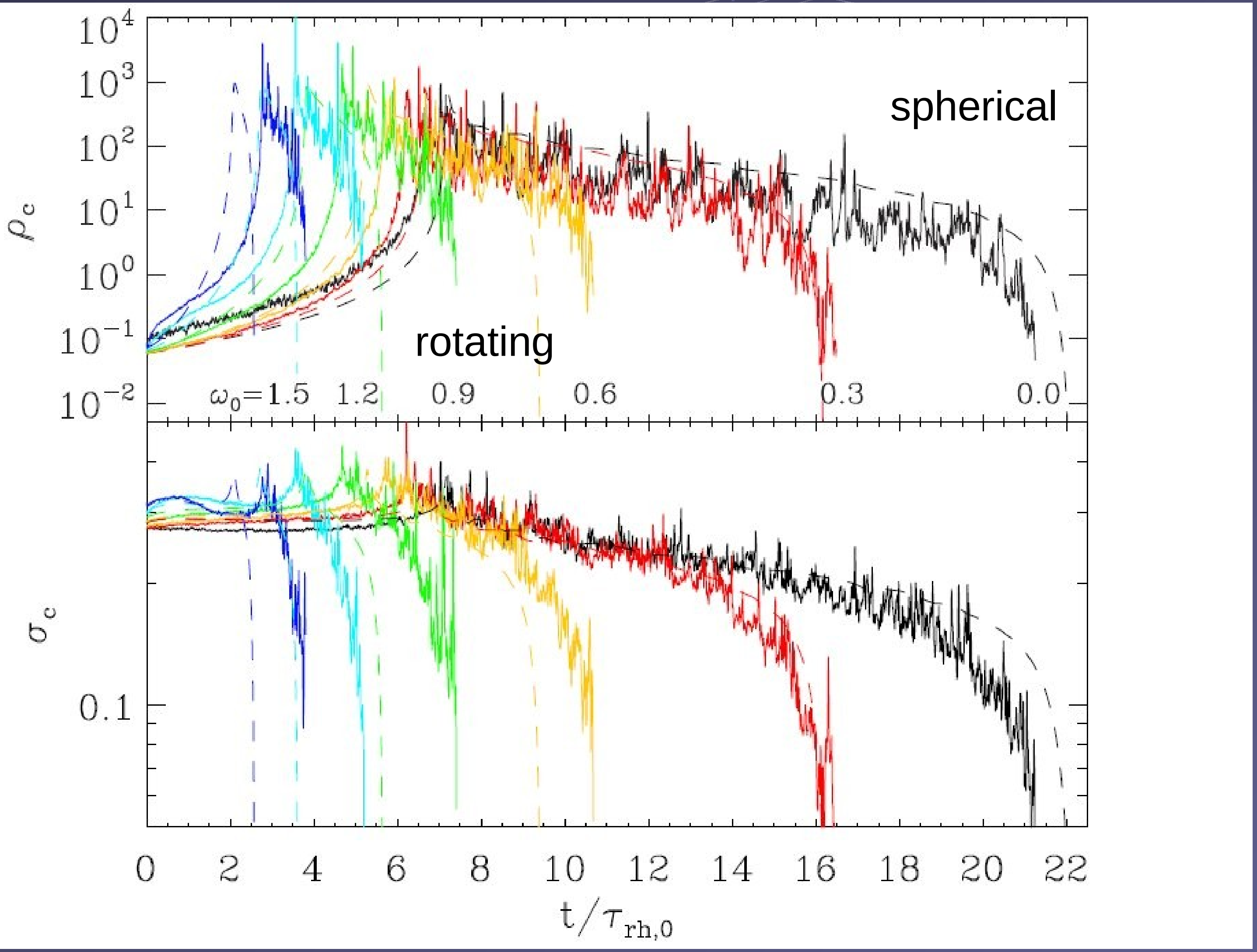

Kim, Yoon, Lee, Spurzem, 2008, MNRAS

Hong, Kim, Lee, Spurzem, 2013, MNRAS

Three Phases in Cluster Dissolution:

1) Core Collapse (Encounters)

2) Post-Collapse Steady Evaporation (Encount)

3) Dynamic final dissolution

VolkswagenStiftung

GRACE Cluster

4 Tflops (32 micro-GRAPE6)
Dual Port Infiniband
4 MPRACE-1 reconfigurable
(soon: 32 MPRACE-2)

GRAPE + MPRACE
= GRACE

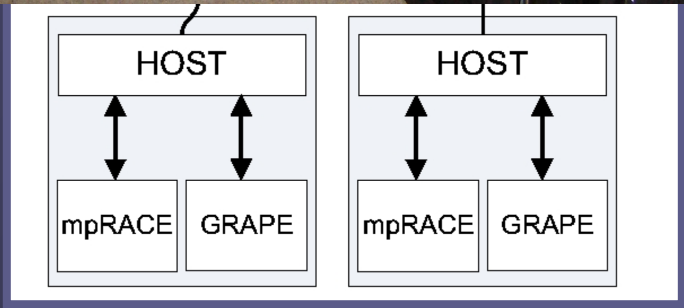

Kupi, G., Amaro-Seoane, P., Spurzem, R., Dynamics of compact object clusters: a post-Newtonian study, 2006, MNRAS 371, L45

Berentzen, I., Preto, M., Berczik, P., Merritt, D., Spurzem, R., Binary Black Hole Merger in Galactic Nuclei: Post-Newtonian Simulations, 2009, ApJ 695, 455

ING / Nr. 32 Seite 5 HEIDELBERGER NACHRICHTEN Mittwoch, 8. Februar 2006

Super-Rechner spürt Schwarzen Löchern nach

Astronomisches Rechen-Institut stellte mit „Grace" einen der schnellsten Rechnern der Welt vor – 3200 Milliarden Rechenoperationen pro Sekunde

Von Harald Berlinghof

Schon ein ganz durchschnittliches dieser gefräßigen, schwarzen Ungeheuer des Universums, die oft in den Zentren der Galaxien hausen, wäre ein furchteinflößendes Etwas, könnten wir ihm je begegnen. Sie sind zwar dunkle Mysterien des Kosmos, doch unnahbar sind sie nicht. Vielmehr zerren sie sogar gerne alles an sich, um es sich einzuverleiben. Schwarze Löcher sind ausgepowerte, kollabierte Sterne, deren Brennstoff nicht mehr ausreicht, um sie strahlen zu lassen. Unter ihrem eigenen Gewicht brechen sie in sich zusammen und bilden eine gewaltige Masse, die solche Gravitationskräfte ausübt, dass nichts, was einmal den sogenannten Ereignishorizont überschritten hat, je wieder zurück kehren kann – noch nicht einmal Licht.

Wie gesagt, dies gilt für ganz normale Schwarze Löcher. Im Astronomischen Rechen-Institut (ARI) der Universität Heidelberg wagt man sich aber inzwischen sogar an sogenannte „supermassive Schwarze Löcher" heran – rein rechnerisch natürlich. „Das sind Schwarze Löcher mit einer Masse vom mindestens einer Million Sonnenmassen und der Größe unseres gesamten Sonnensystems", erklärt Professor Rainer Spurzem vom ARI.

In Computersimulationen wird berechnet, was passiert, wenn zwei Galaxien, die solche supermassiven Schwarzen Löcher in sich tragen, miteinander kollidieren. Millionen von Sonnen und Planetensystemen kommen sich dann so nahe, dass die gegenseitigen Anziehungskräfte die jeweiligen Bahnen der Sonnen verändern und beide Galaxien in starke Drehbewegungen und rotierende Verwirbelungen versetzen. Aus den beiden kollidierten Spiralgalaxien entstehen kurzzeitig – für wenige Millionen Jahre – sogenannte Antennengalaxien – so bezeichnet wegen ihrer Form.

Berechnen muss man solche hochkomplexen Ereignisse freilich mit einem Superrechner. Und im Astronomischen Rechen-Institut hat man mit der finanziellen Hilfe der Volkswagenstiftung, der Deutschen Forschungsgemeinschaft und dem Land Baden-Württemberg sowie des Hardware-Know-Hows der Informatik der Mannheimer Universität am Lehrstuhl von Professor Reinhard Männer aus 32 Hochleistungs-PCs einen Top-50-Rechner namens „Grace" konstruiert, der zu den schnellsten Rechnern der Welt zählt.

So richtig schnell machen ihn spezielle Grafikkarten namens „Grape" aus Japan und solche aus Mannheim mit Namen „MPRace". 3200 Milliarden Rechenoperationen in der Sekunde sind die Folge. „Ein Rechner für 20 Millionen Euro bringt auch nicht mehr", so Spurzem. Allerdings schafft es Grace nicht in die Weltrangliste der schnellsten Rechner, weil er ein Spezialist ist, der nur auf dem Problem der Gravitationsberechnung funktioniert. In anderen Bereichen würde er kläglich versagen.

Im Jahr 1937, also bevor Computersimulationen möglich waren, weil Konrad Zuse den Computer erst später erdachte, hatte der Forscher Erk Holmberg die Entstehung der „Antennengalaxien" beim Zusammenstoß zweier Spiralgalaxien bereits aufgezeigt. Seine mechanische Methode brachte ein ähnliches Ergebnis hervor wie der Rechner „Grace". Doch „Grace" hat noch etwas anderes berechnet. Der Zusammenschluss zweier supermassiver Schwarzer Löcher erfolgt viel schneller als bisher vermutet – sie benötigen nur rund 100 Millionen Jahre, um zu verschmelzen und dabei starke Gravitationswellen auszusenden. Könnte man die Gravitationswellen nachweisen, wäre der letzte große Lückenschluss in Einsteins Relativitätstheorie gelungen.

Am Astronomischen Recheninstitut stellten Mitarbeiter ihren neuen schnellen Rechner vor, der auf der Suche nach den Gravitationswellen helfen soll. Von der Rechenkraft gehört er in die Top 50 der schnellsten Rechner auf der Welt, obwohl er nur aus einfachen PCs zusammengebaut ist. Foto: Kresin

Miro „schnappt" zwei Einbrecher

Der Polizeihund erschnüffelte in Wieblingen die Männer, die sich im Keller versteckt hatten

POLIZEIBERICHT

VolkswagenStiftung

1) Introduction – History

2) Star Cluster Dynamics with Black Holes and gravitational waves

1) Star Clusters with IMBH formation

2) Code(s) and Hardware

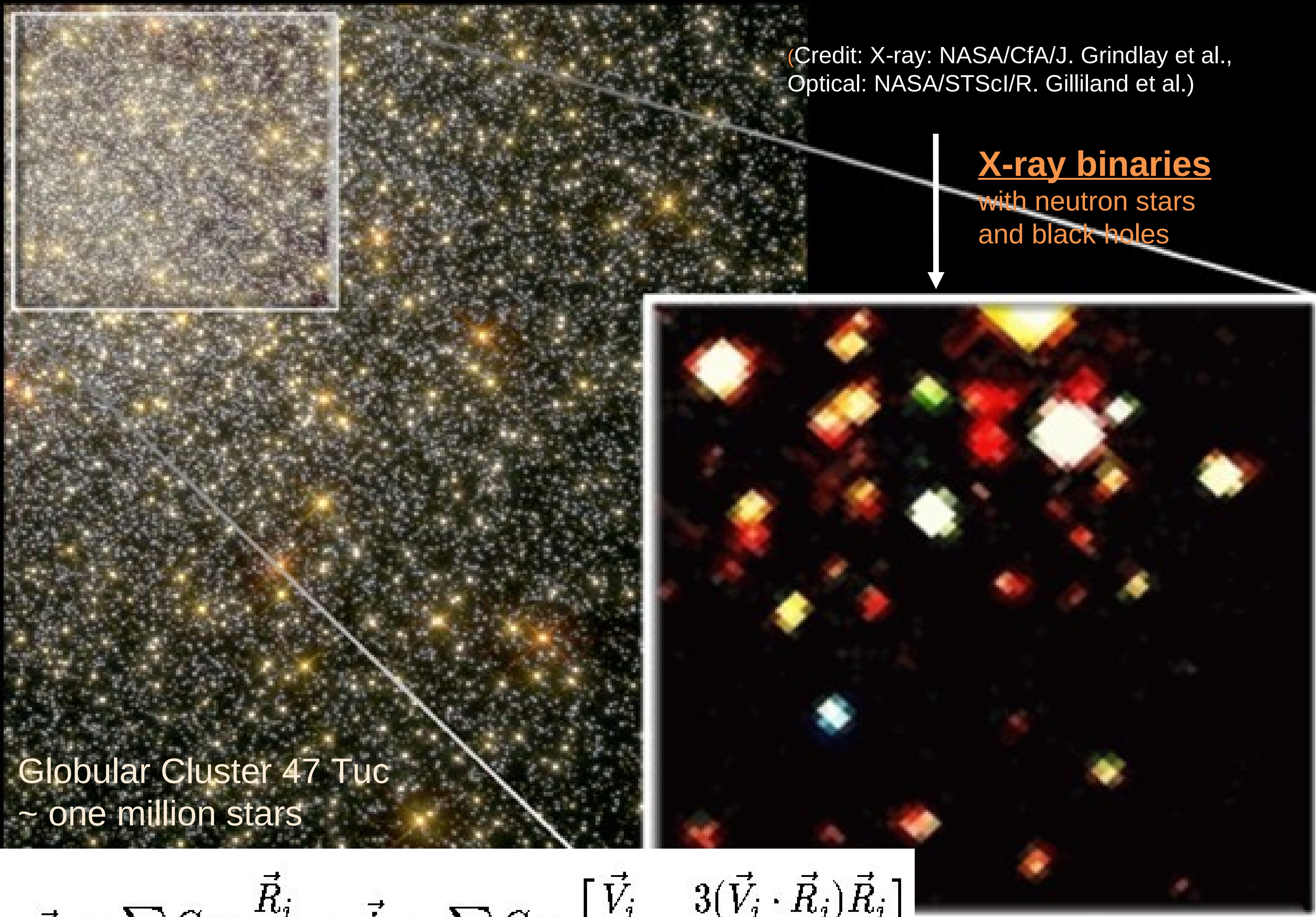

$$\vec{a}_0 = \sum_j G m_j \frac{\vec{R}_j}{R_j^3} \quad ; \quad \dot{\vec{a}}_0 = \sum_j G m_j \left[\frac{\vec{V}_j}{R_j^3} - \frac{3(\vec{V}_j \cdot \vec{R}_j)\vec{R}_j}{R_j^5} \right]$$

DRAGON Simulation

http://silkroad.bao.ac.cn/dragon/

One million stars direct simulation,

biggest and most realistic direct N-Body simulation of globular star clusters.
With stellar mass function, single and binary stellar evolution, regularization of close encounters, tidal field (NBODY6++GPU).
(NAOC/Silk Road/MPA collaboration).

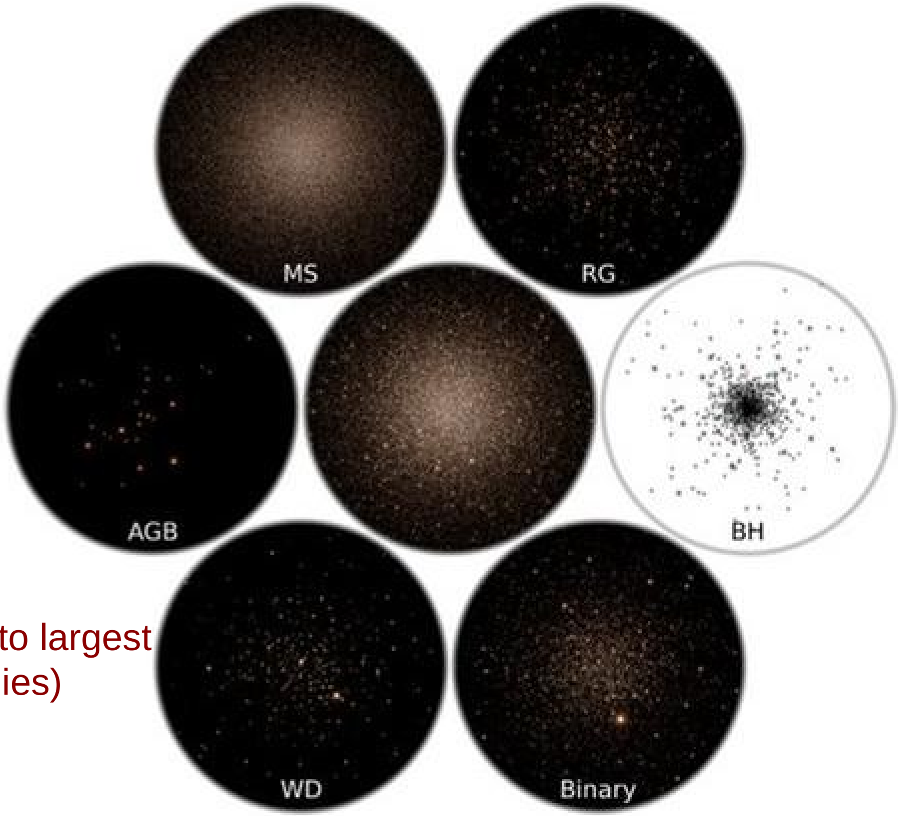

Wang, Spurzem, Aarseth, Naab et al. MNRAS, 2015
Wang, Spurzem, Aarseth Naab, et al. MNRAS 2016

Number of Floating Point Operations (~1M bodies) similar to largest Cosmological simulations (Millennium, Illustris, ~100M bodies)

天龙星团模拟：百万数量级恒星、黑洞和引力波

Dragon Star Cluster Simulations: Millions of Stars; black holes and gravitational waves

- First realistic globular star cluster model with million stars *(Wang, Spurzem, Aarseth, …, Berczik, Kouwenhoven, … MNRAS 2015, 2016)*
- Synthetic CMD (right side) with zero photometric errors, different ages shown
- Black hole binary mergers occur as observed by LIGO. Our grav. waveforms computed from simulation (right side). (Only inspiral plotted not ringdown.)
- GPU accelerated supercomputers laohu in NAOC and hydra of Max-Planck (MPCDF) in Germany needed!

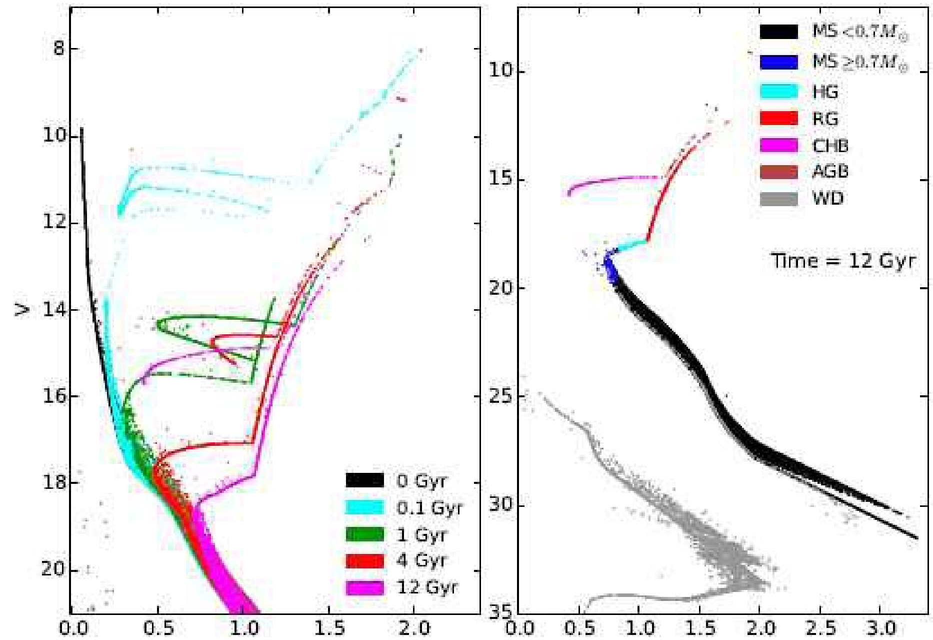

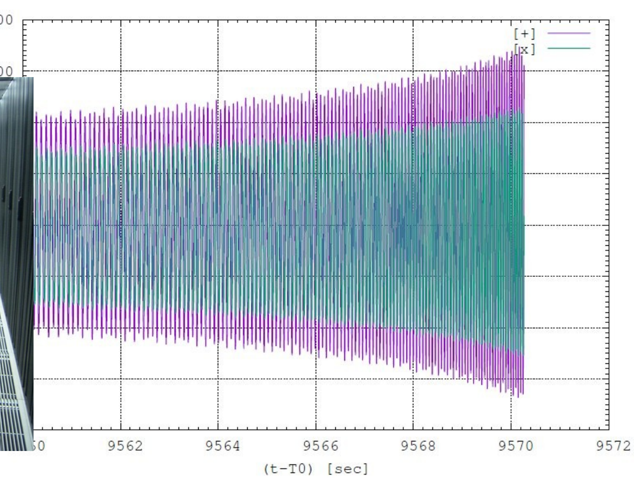

http://www.mpa-garching.mpg.de/328833/hl201603

CPU/GPU N-body6++

Leiden

Key Question 1. When will we see the first star-by-star *N*-body model of a globular cluster?

- Honest N-body simulation
- Reasonable mass at 12 Gyr (~$5 \times 10^4 M_\odot$)
- Reasonable tide (circular galactic orbit will do)
- Reasonable IMF (e.g. Kroupa)
- Reasonable binary fraction (a few percent)
- Any initial model you like (Plummer will do)
- A submitted paper (astro-ph will do)

An inducement: a bottle of single malt Scotch whisky worth €50

Long Wang, Ph.D. Peking University 2016:
Million-Body Award by MODEST community
And IAU Ph.D. prize

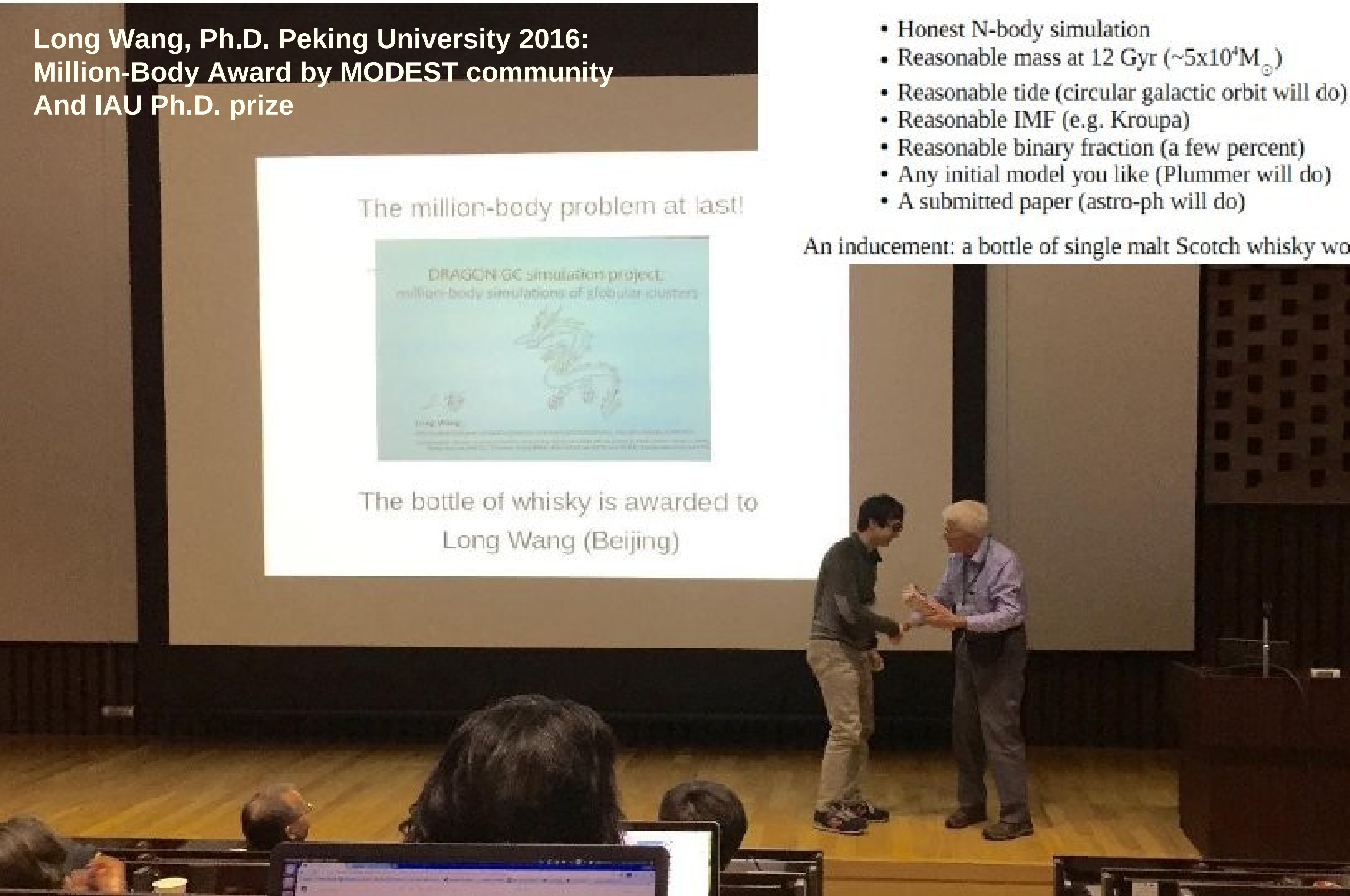

CPU/GPU N-body6++

Our Team Re-Union at MODEST-15s in Kobe, Dec. 2015
(ARI Heidelberg around 2000)

Gong, Lau, … Spurzem … 2015, 2011 (JphCS, CQGra)

Background Plot: Sesana 2016

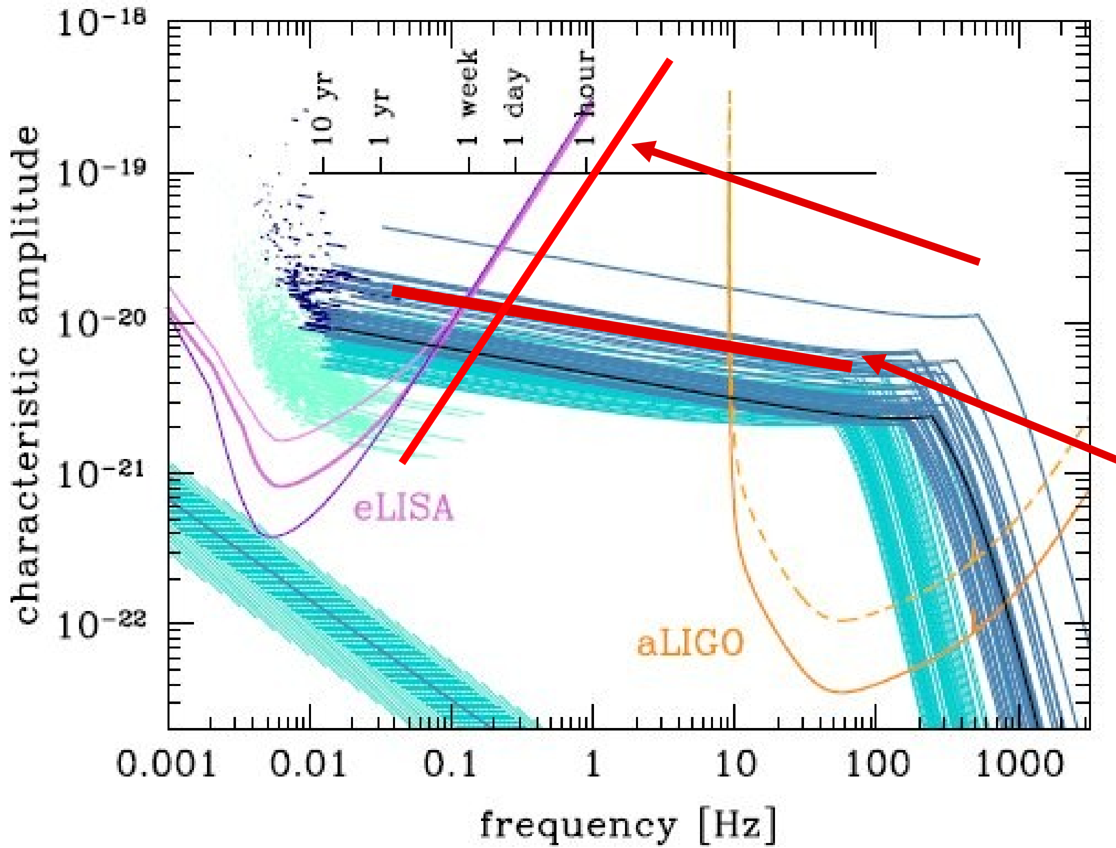

Taiji or Tianqin Hand Drawn Estimate

"Our" DRAGON Black Hole Binary

FIG. 1: The multi-band GW astronomy concept. The violet lines are the total sensitivity curves (assuming two Michelson) of three eLISA configurations; from top to bottom N2A1, N2A2, N2A5 (from [11]). The orange lines are the current (dashed) and design (solid) aLIGO sensitivity curves. The lines in different blue flavours represent characteristic amplitude tracks of BHB sources for a realization of the *flat* population model (see main text) seen with S/N> 1 in the N2A2 configuration (highlighted as the thick eLISA middle curve), integrated assuming a five year mission lifetime. The light turquoise lines clustering around 0.01Hz are sources seen in eLISA with S/N< 5 (for clarity, we down-sampled them by a factor of 20 and we removed sources extending to the aLIGO band); the light and dark blue curves crossing to the aLIGO band are sources with S/N> 5 and S/N> 8 respectively in eLISA; the dark blue marks in the upper left corner are other sources with S/N> 8 in eLISA but not crossing to the aLIGO band within the mission lifetime. For comparison, the characteristic amplitude track completed by GW150914 is shown as a black solid line, and the chart at the top of the figure indicates the frequency progression of this particular source in the last 10 years before coalescence. The shaded area at the bottom left marks the expected confusion noise level produced by the same population model (median, 68% and 95% intervals are shown). The waveforms shown are second order post-Newtonian inspirals phenomenologically adjusted with a Lorentzian function to describe the ringdown.

Post-Newtonian Dynamics

r;v : relative distance, velocity
$\mu = m_1 m_2 / M$: reduced mass ($M = m_1 + m_2$)
$\nu = \mu / M$: mass ratio
n = **r** / r : unit vector in radial direction

$$\frac{dv^i}{dt} = -\frac{Gm}{r^2}\left[(1+\mathcal{A})\,n^i + \mathcal{B}\,v^i\right] + \mathcal{O}\left(\frac{1}{c^8}\right), \qquad (181)$$

and find [43] that the coefficients $\mathcal{A}$ and $\mathcal{B}$ are

$$\mathcal{A} = \frac{1}{c^2}\left\{-\frac{3\dot{r}^2\nu}{2} + v^2 + 3\nu v^2 - \frac{Gm}{r}(4+2\nu)\right\}$$

Perihel shift

$$+\frac{1}{c^4}\left\{\frac{15\dot{r}^4\nu}{8} - \frac{45\dot{r}^4\nu^2}{8} - \frac{9\dot{r}^2\nu v^2}{2} + 6\dot{r}^2\nu^2 v^2 + 3\nu v^4 - 4\nu^2 v^4\right.$$

... higher order…

$$\left. + \frac{Gm}{r}\left(-2\dot{r}^2 - 25\dot{r}^2\nu - 2\dot{r}^2\nu^2 - \frac{13\nu v^2}{2} + 2\nu^2 v^2\right) + \frac{G^2m^2}{r^2}\left(9 + \frac{87\nu}{4}\right)\right\}$$

$$+\frac{1}{c^5}\left\{-\frac{24\dot{r}\nu v^2}{5}\frac{Gm}{r} - \frac{136\dot{r}\nu}{15}\frac{G^2m^2}{r^2}\right\}$$

Grav. Radiation

Schäfer, Gauge Theor. Grav. 36, 2223 (2004)
Memmesheimer, Gopakumar, Schäfer, Phys. Rev.D 70, 104011 (2004)
Blanchet, Luc; Living Reviews 2002, llr-2002-3

$$
\begin{aligned}
&+\frac{1}{c^6}\Bigg\{-\frac{35\dot{r}^6\nu}{16}+\frac{175\dot{r}^6\nu^2}{16}-\frac{175\dot{r}^6\nu^3}{16}+\frac{15\dot{r}^4\nu v^2}{2}-\frac{135\dot{r}^4\nu^2v^2}{4}+\frac{255\dot{r}^4\nu^3v^2}{8}\\
&\qquad-\frac{15\dot{r}^2\nu v^4}{2}+\frac{237\dot{r}^2\nu^2v^4}{8}-\frac{45\dot{r}^2\nu^3v^4}{2}+\frac{11\nu v^6}{4}-\frac{49\nu^2v^6}{4}+13\nu^3v^6\\
&\qquad+\frac{Gm}{r}\Bigg(79\dot{r}^4\nu-\frac{69\dot{r}^4\nu^2}{2}-30\dot{r}^4\nu^3-121\dot{r}^2\nu v^2+16\dot{r}^2\nu^2v^2+20\dot{r}^2\nu^3v^2+\frac{75\nu v^4}{4}\\
&\qquad\qquad+8\nu^2v^4-10\nu^3v^4\Bigg)\\
&\qquad+\frac{G^2m^2}{r^2}\Bigg(\dot{r}^2+\frac{32573\dot{r}^2\nu}{168}+\frac{11\dot{r}^2\nu^2}{8}-7\dot{r}^2\nu^3+\frac{615\dot{r}^2\nu\pi^2}{64}-\frac{26987\nu v^2}{840}+\nu^3v^2\\
&\qquad\qquad-\frac{123\nu\pi^2v^2}{64}-110\dot{r}^2\nu\ln\left(\frac{r}{r_0'}\right)+22\nu v^2\ln\left(\frac{r}{r_0'}\right)\Bigg)\\
&\qquad+\frac{G^3m^3}{r^3}\left(-16-\frac{437\nu}{4}-\frac{71\nu^2}{2}+\frac{41\nu\pi^2}{16}\right)\Bigg\}\\
&+\frac{1}{c^7}\Bigg\{\frac{Gm}{r}\left(\frac{366}{35}\nu v^4+12\nu^2v^4-114v^2\nu\dot{r}^2-12\nu^2v^2\dot{r}^2+112\nu\dot{r}^4\right)\\
&\qquad+\frac{G^2m^2}{r^2}\left(\frac{692}{35}\nu v^2-\frac{724}{15}v^2\nu^2+\frac{294}{5}\nu\dot{r}^2+\frac{376}{5}\nu^2\dot{r}^2\right)\\
&\qquad+\frac{G^3m^3}{r^3}\left(\frac{3956}{35}\nu+\frac{184}{5}\nu^2\right)\Bigg\},
\end{aligned}
\tag{182}
$$

$$
\begin{aligned}
\mathcal{B} = {}& \frac{1}{c^2}\left\{-4\dot{r} + 2\dot{r}\nu\right\} \\
&+ \frac{1}{c^4}\left\{\frac{9\dot{r}^3\nu}{2} + 3\dot{r}^3\nu^2 - \frac{15\dot{r}\nu v^2}{2} - 2\dot{r}\nu^2 v^2 + \frac{Gm}{r}\left(2\dot{r} + \frac{41\dot{r}\nu}{2} + 4\dot{r}\nu^2\right)\right\} \\
&+ \frac{1}{c^5}\left\{\frac{8\nu v^2}{5}\frac{Gm}{r} + \frac{24\nu}{5}\frac{G^2m^2}{r^2}\right\} \\
&+ \frac{1}{c^6}\left\{-\frac{45\dot{r}^5\nu}{8} + 15\dot{r}^5\nu^2 + \frac{15\dot{r}^5\nu^3}{4} + 12\dot{r}^3\nu v^2 - \frac{111\dot{r}^3\nu^2 v^2}{4} - 12\dot{r}^3\nu^3 v^2 - \frac{65\dot{r}\nu v^4}{8}\right. \\
&\qquad + 19\dot{r}\nu^2 v^4 + 6\dot{r}\nu^3 v^4 \\
&\qquad + \frac{Gm}{r}\left(\frac{329\dot{r}^3\nu}{6} + \frac{59\dot{r}^3\nu^2}{2} + 18\dot{r}^3\nu^3 - 15\dot{r}\nu v^2 - 27\dot{r}\nu^2 v^2 - 10\dot{r}\nu^3 v^2\right) \\
&\qquad \left. + \frac{G^2m^2}{r^2}\left(-4\dot{r} - \frac{18169\dot{r}\nu}{840} + 25\dot{r}\nu^2 + 8\dot{r}\nu^3 - \frac{123\dot{r}\nu\pi^2}{32} + 44\dot{r}\nu\ln\left(\frac{r}{r'_0}\right)\right)\right\} \\
&+ \frac{1}{c^7}\left\{\frac{Gm}{r}\left(-\frac{626}{35}\nu v^4 - \frac{12}{5}\nu^2 v^4 + \frac{678}{5}\nu v^2\dot{r}^2 + \frac{12}{5}\nu^2 v^2\dot{r}^2 - 120\nu\dot{r}^4\right)\right. \\
&\qquad + \frac{G^2m^2}{r^2}\left(\frac{164}{21}\nu v^2 + \frac{148}{5}\nu^2 v^2 - \frac{82}{3}\nu\dot{r}^2 - \frac{848}{15}\nu^2\dot{r}^2\right) \\
&\qquad \left. + \frac{G^3m^3}{r^3}\left(-\frac{1060}{21}\nu - \frac{104}{5}\nu^2\right)\right\}. \qquad (183)
\end{aligned}
$$

Gravitational Waves

What happens afterwards? Post-Newton Order „2.5“...

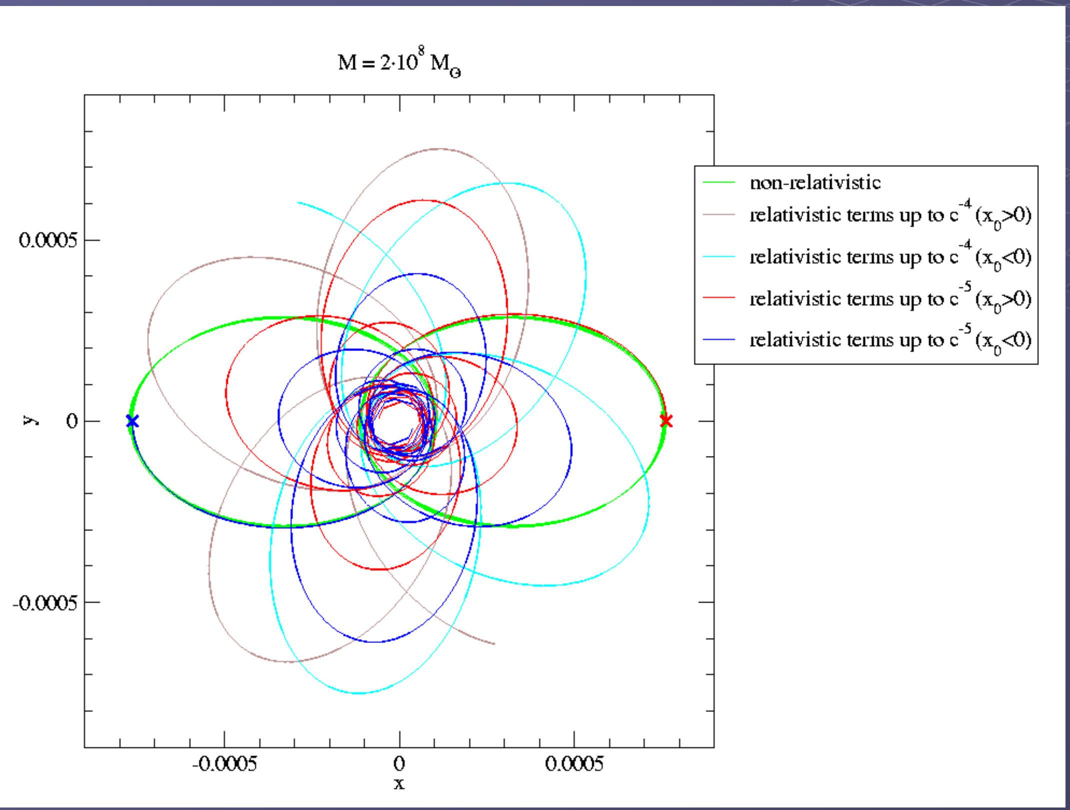

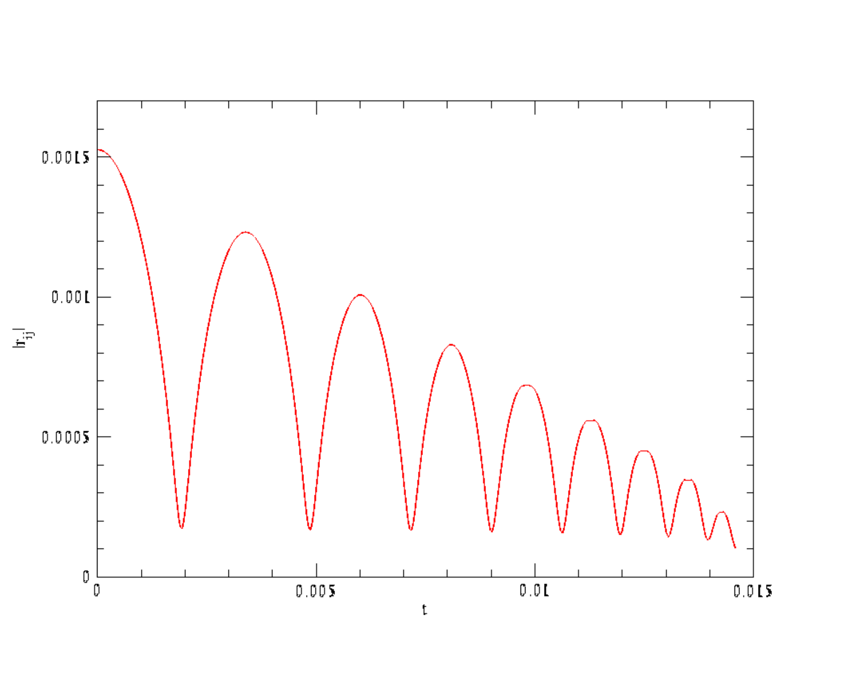

Kupi, Amaro-Seoane & Spurzem 2006

Indirect Proof by Hulse and Taylor, binary pulsar (Nobel prize 1993)

"for the discovery of a new type of pulsar, a discovery that has opened up new possibilities for the study of gravitation"

Comparison between observations of the binary pulsar PSR1913+16, and the prediction of general relativity based on loss of orbital energy via gravitational waves

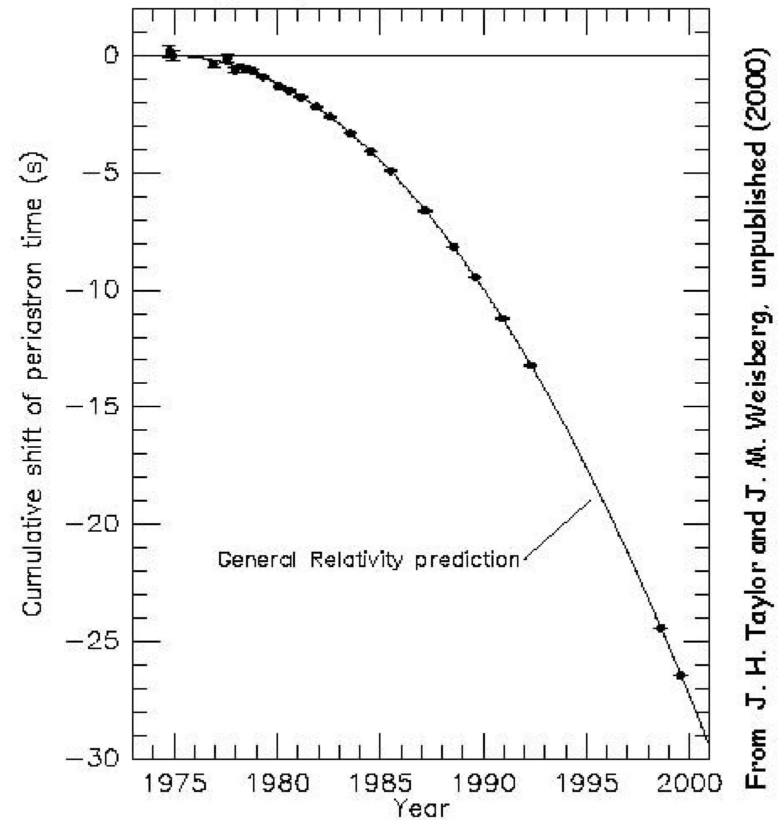

Gravitational Waves: Degree of Complexity

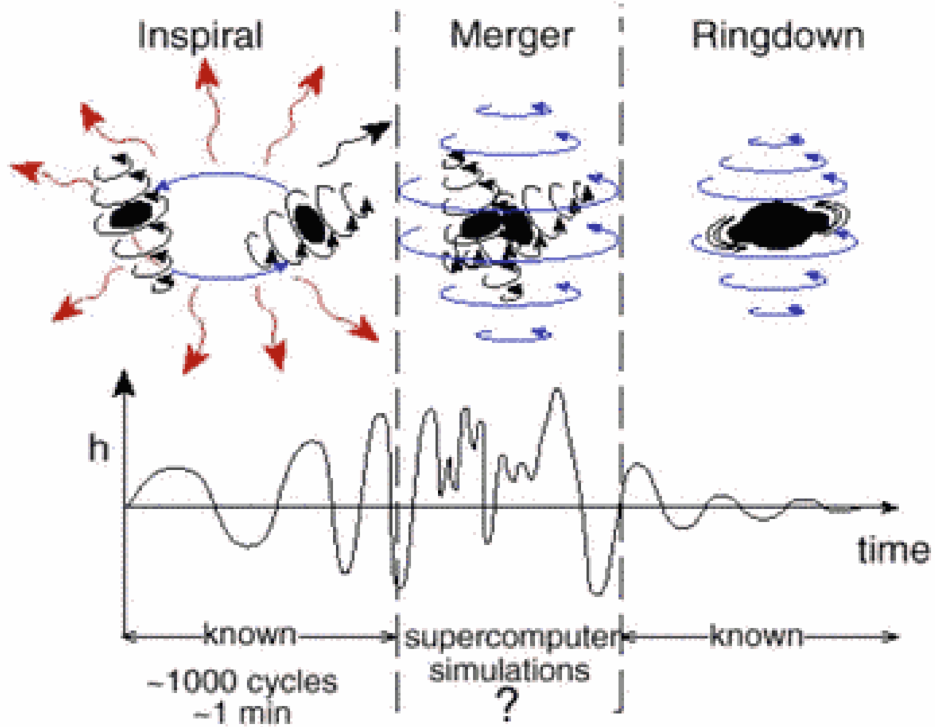

Slide by P. Laguna

Is this the right picture?

So far, it seems not!

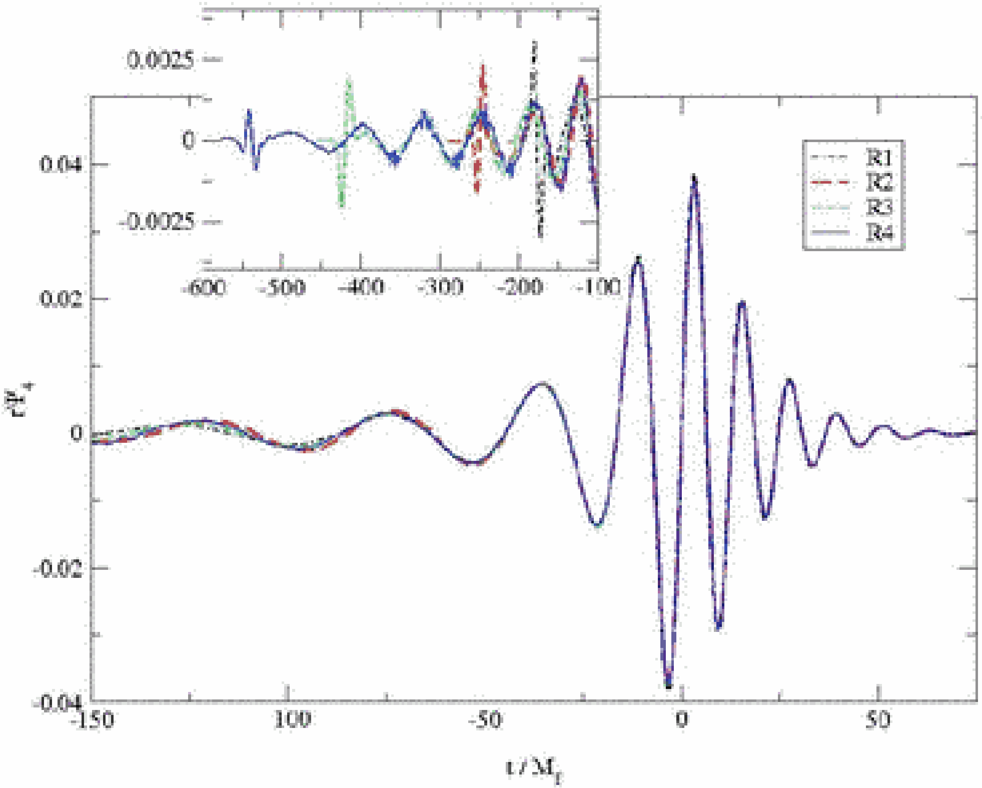

Initial separations:
R1 = 6.5 M
R2 = 7.6 M
R3 = 8.5 M
R4 = 9.6 M

NASA-GSFC
Baker, Centrella, Choi, Koppitz, van Meter
Phys.Rev. D73 (2006) 104002

Slide by P. Laguna

Post-Newtonian Dynamics

Spin-Orbit Interaction S / Spin-Spin SS

$$\frac{d\mathbf{v}_1}{dt} = \mathbf{A}_{\mathrm{N}} + \frac{1}{c^2}\mathbf{A}_{1\mathrm{PN}} + \frac{1}{c^3}\underset{\mathrm{S}}{\mathbf{A}}_{1.5\mathrm{PN}} + \frac{1}{c^4}\left[\mathbf{A}_{2\mathrm{PN}} + \underset{\mathrm{SS}}{\mathbf{A}}_{2\mathrm{PN}}\right] + \frac{1}{c^5}\left[\mathbf{A}_{2.5\mathrm{PN}} + \underset{\mathrm{S}}{\mathbf{A}}_{2.5\mathrm{PN}}\right] + \mathcal{O}\left(\frac{1}{c^6}\right). \qquad (5.1)$$

Faye, Blanchet, Buonanno 2006

$$\underset{\mathrm{S}}{\mathbf{A}}_{1.5\mathrm{PN}} = \frac{Gm_2}{r_{12}^3}\left\{\left[6\frac{(S_1, n_{12}, v_{12})}{m_1} + 6\frac{(S_2, n_{12}, v_{12})}{m_2}\right]\mathbf{n}_{12} + 3(n_{12}v_{12})\frac{\mathbf{n}_{12}\times\mathbf{S}_1}{m_1} + 6(n_{12}v_{12})\frac{\mathbf{n}_{12}\times\mathbf{S}_2}{m_2} - 3\frac{\mathbf{v}_{12}\times\mathbf{S}_1}{m_1} - 4\frac{\mathbf{v}_{12}\times\mathbf{S}_2}{m_2}\right\}. \qquad (5.3a)$$

Rezzolla
Final Spin
Formula

Brem,
Amaro-Seoane,
Spurzem,
MNRAS 2013

$$|\mathbf{a}_{\rm fin}| = \frac{1}{(1+q)^2}\Big[|\mathbf{a}_1|^2 + |\mathbf{a}_2|^2 q^4 + 2|\mathbf{a}_2||\mathbf{a}_1|q^2 \cos\alpha + 2(|\mathbf{a}_1|\cos\beta + |\mathbf{a}_2|q^2\cos\gamma)|\mathbf{l}|q + |\mathbf{l}|^2 q^2\Big]^{1/2},$$

where $q = M_2/M_1$ is the mass ratio and the angles are defined as

$$\cos\alpha = \hat{a}_1 \cdot \hat{a}_2, \qquad \cos\beta = \hat{a}_1 \cdot \hat{l}, \qquad \cos\gamma = \hat{a}_2 \cdot \hat{l}.$$

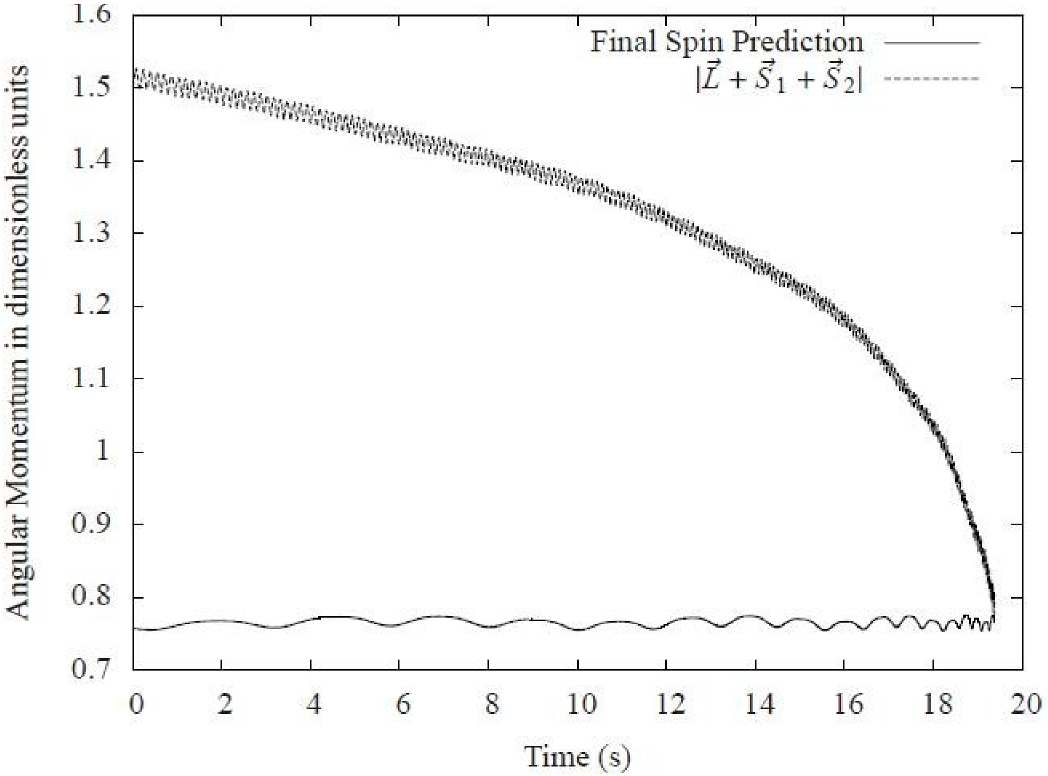

Figure 3.7: Comparison between the current final spin prediction and the actual total angular momentum of the binary system.

Post-Newtonian Dynamics

Brem, Amaro-Seoane,
Spurzem,
MNRAS 2013

Include
Spin-Orbit
Spin-Spin
PN3, PN3.5
Spin Dynamics

By Patrick Brem
(Diploma Thesis
Univ. Heidelberg)

1PN
2PN + 1.5PN SO
3PN + 2.5PN SO
2.5PN + 2PN SS
3.5PN

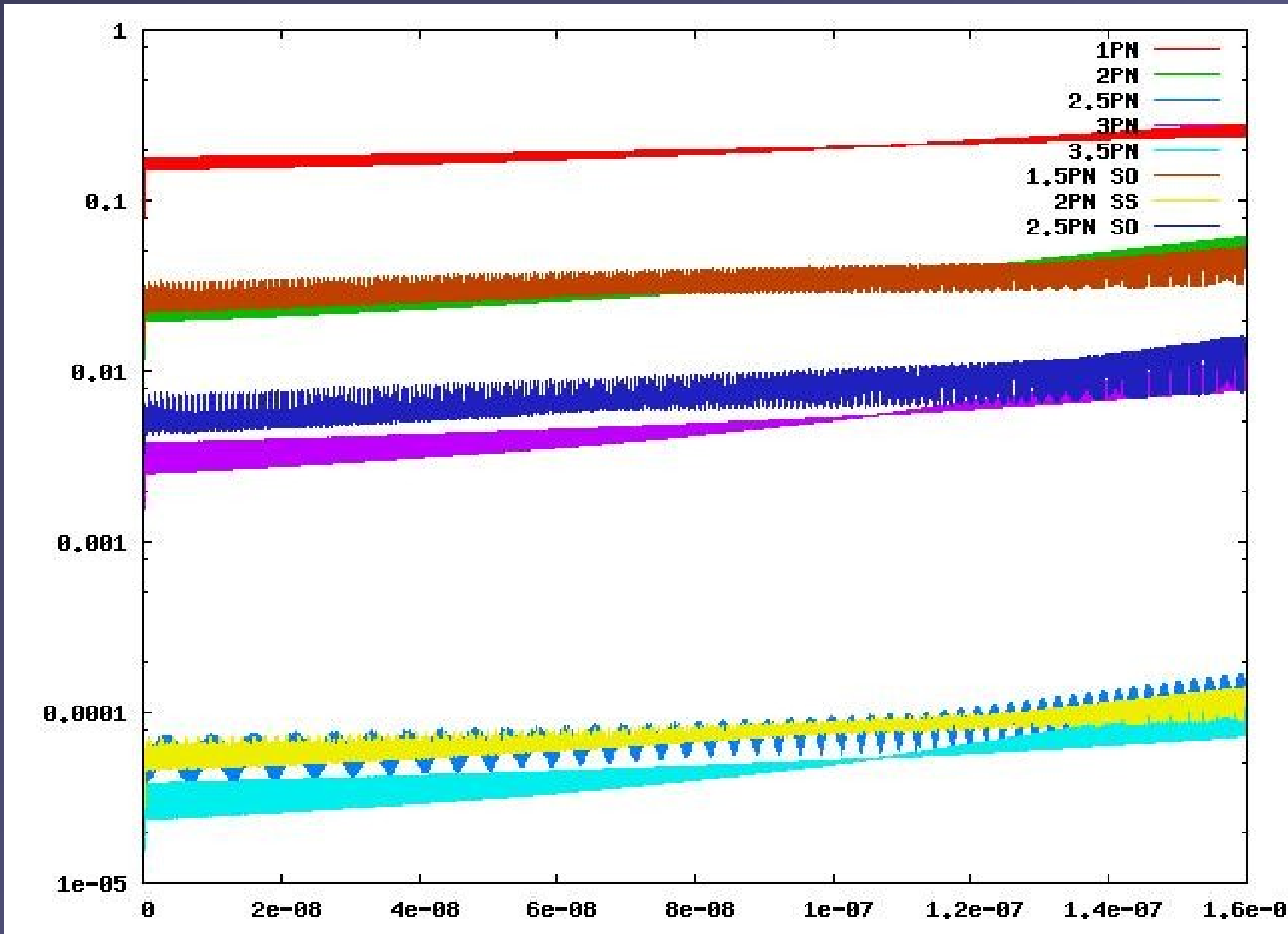

Post-Newtonian Dynamics Gravitational Wave Templates

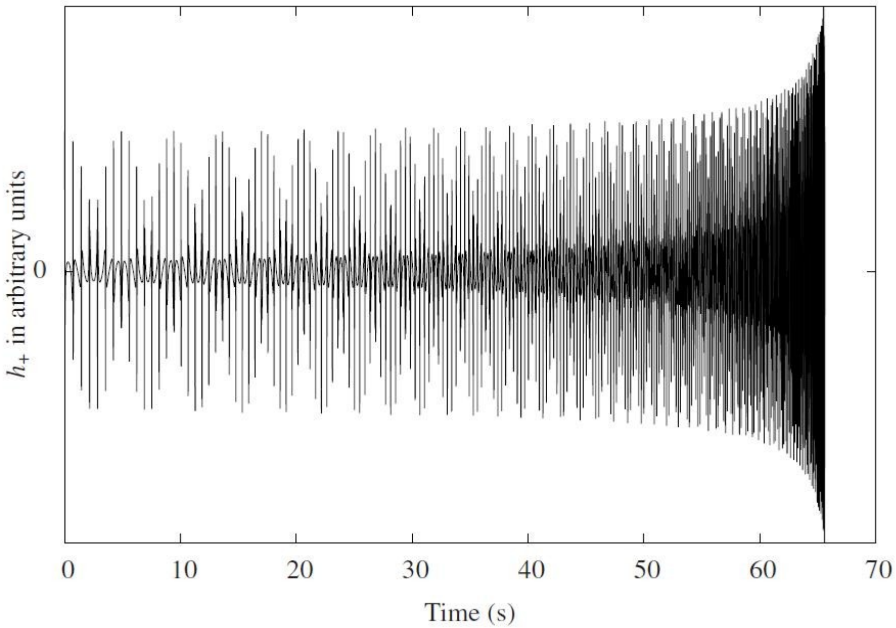

Figure 3.11: Waveform for two equal mass objects on a an orbit with $e = 0.5$.

Brem,
Amaro-Seoane,
Spurzem,
MNRAS 2013

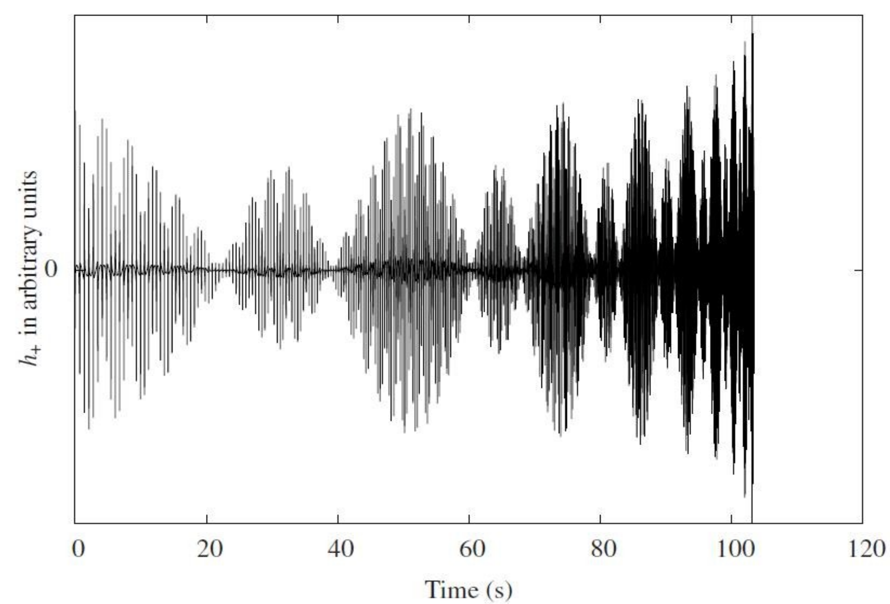

Figure 3.12: Waveform for two objects with a mass ratio of $q = 1/10$ on an orbit with $e = 0.5$ and spins $a_{1,x} = 1.0$, $a_{2,y} = 1.0$.

Handle spin-orbit and spin-spin coupling
(P.Brem, R. Spurzem, Univ. Heidelberg)

GW Detection Abott et al. 2016

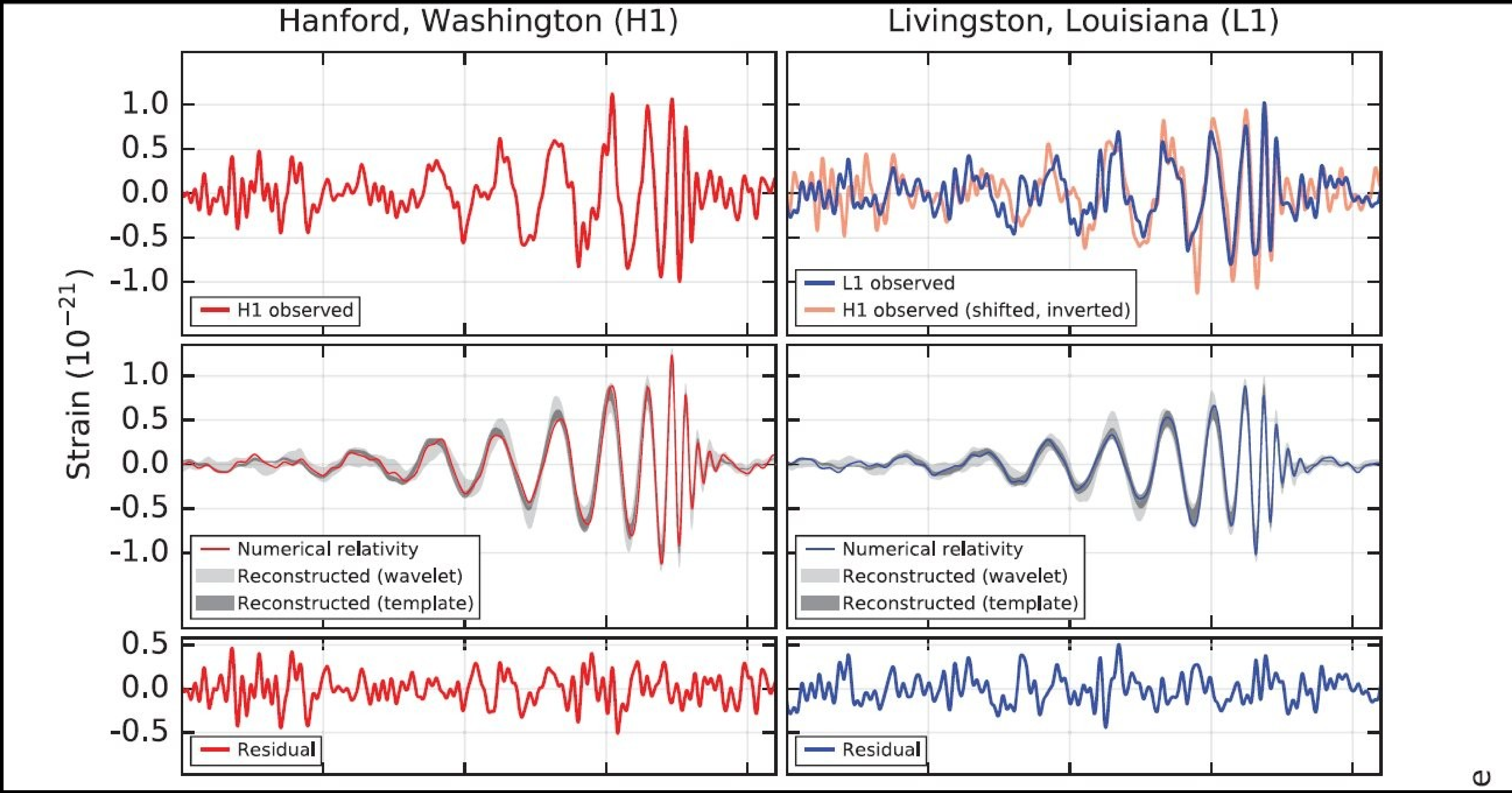

GW Detection Abott et al. 2016

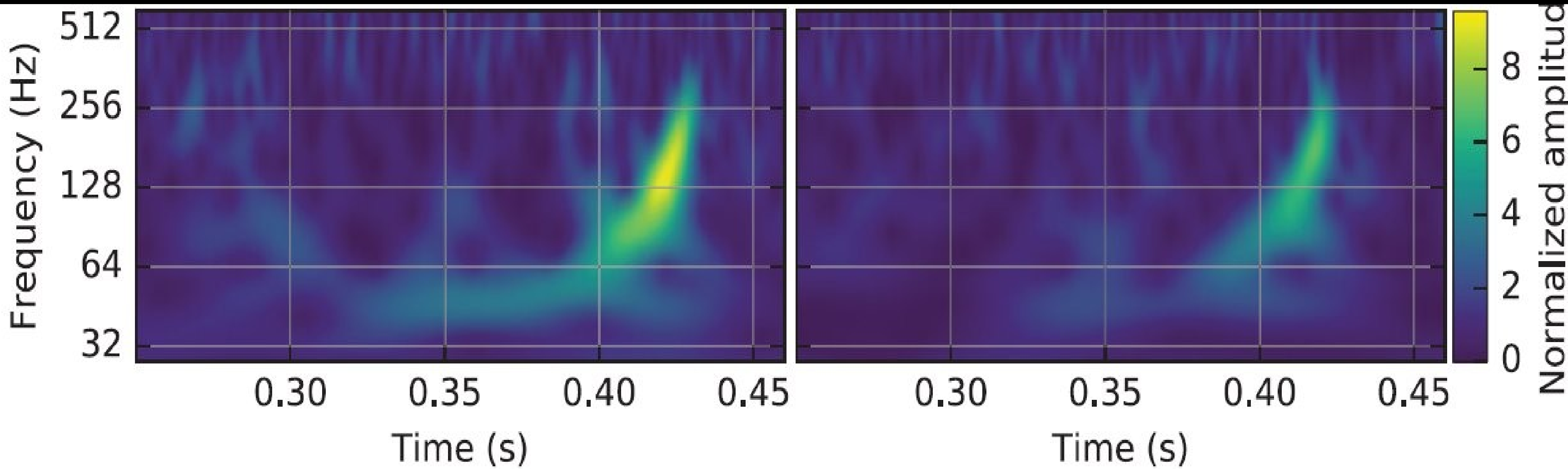

FIG. 1. The gravitational-wave event GW150914 observed by the LIGO Hanford (H1, left column panels) and Livingston (L1, right column panels) detectors. Times are shown relative to September 14, 2015 at 09:50:45 UTC. For visualization, all time series are filtered with a 35–350 Hz bandpass filter to suppress large fluctuations outside the detectors' most sensitive frequency band, and band-reject filters to remove the strong instrumental spectral lines seen in the Fig. 3 spectra. *Top row, left:* H1 strain. *Top row, right:* L1 strain. GW150914 arrived first at L1 and $6.9^{+0.5}_{-0.4}$ ms later at H1; for a visual comparison, the H1 data are also shown, shifted in time by this amount and inverted (to account for the detectors' relative orientations). *Second row:* Gravitational-wave strain projected onto each detector in the 35–350 Hz band. Solid lines show a numerical relativity waveform for a system with parameters consistent with those recovered from GW150914 [37,38] confirmed to 99.9% by an independent calculation based on [15]. Shaded areas show 90% credible regions for two independent waveform reconstructions. One (dark gray) models the signal using binary black hole template waveforms [39]. The other (light gray) does not use an astrophysical model, but instead calculates the strain signal as a linear combination of sine-Gaussian wavelets [40,41]. These reconstructions have a 94% overlap, as shown in [39]. *Third row:* Residuals after subtracting the filtered numerical relativity waveform from the filtered detector time series. *Bottom row:*A time-frequency representation [42] of the strain data, showing the signal frequency increasing over time.

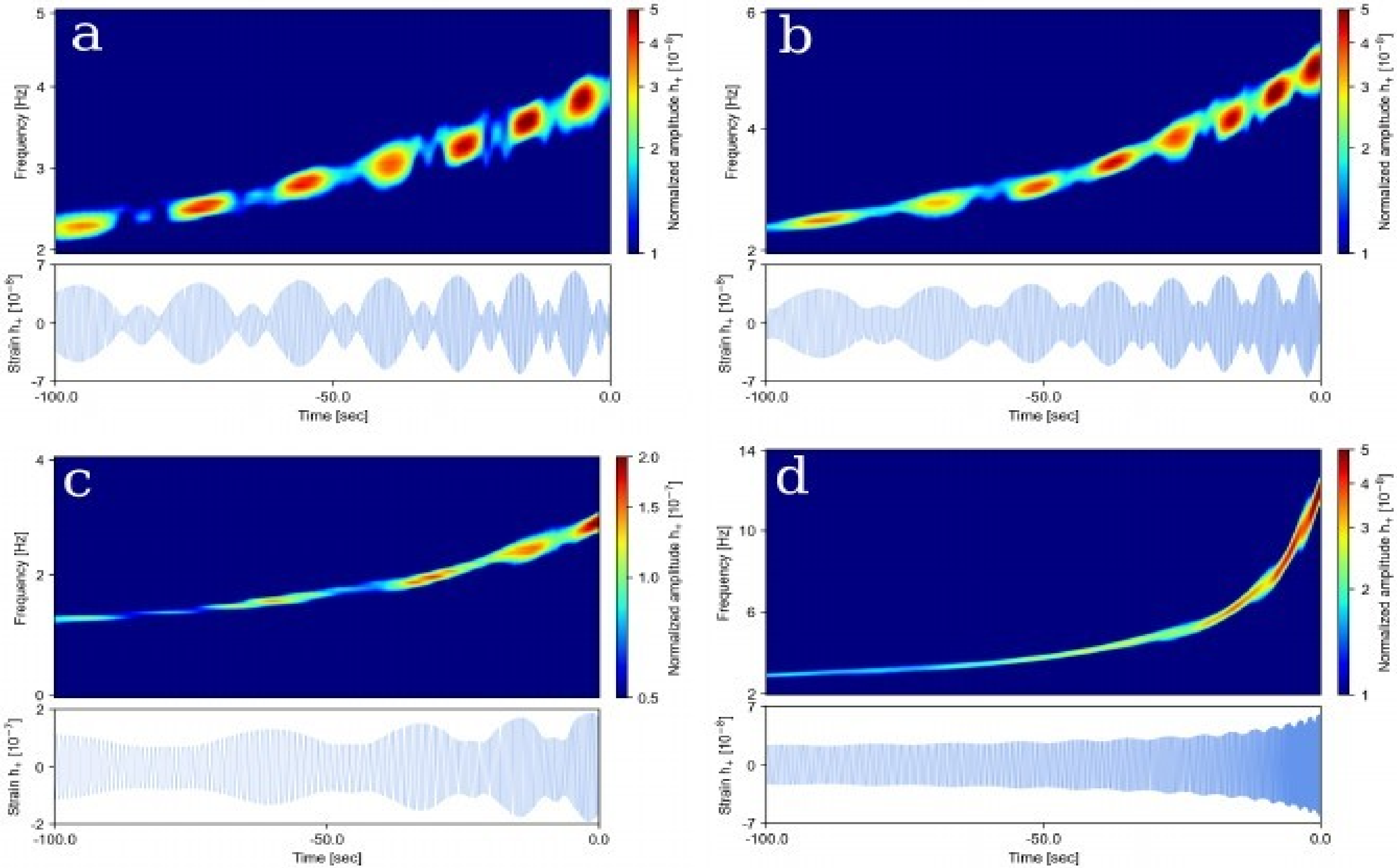

Figure 1. Time-frequency representation (top) of the strain data (bottom) for gravitational waveforms of h_+ polarisation from BBHs (Table 1): (a) - Id 5 ($q = 0.049$), (b) - Id 1 ($q = 0.064$), (c) - Id 6 ($q = 0.167$), (d) - Id 7 ($q = 0.174$). Data are depicted for the last 100 sec of merging. Individual dimensionless spin parameters are $\chi_0 = \chi_1 = [-1, 0, 0]$.

VIRGO Detector in Cascina near Pisa, Italy

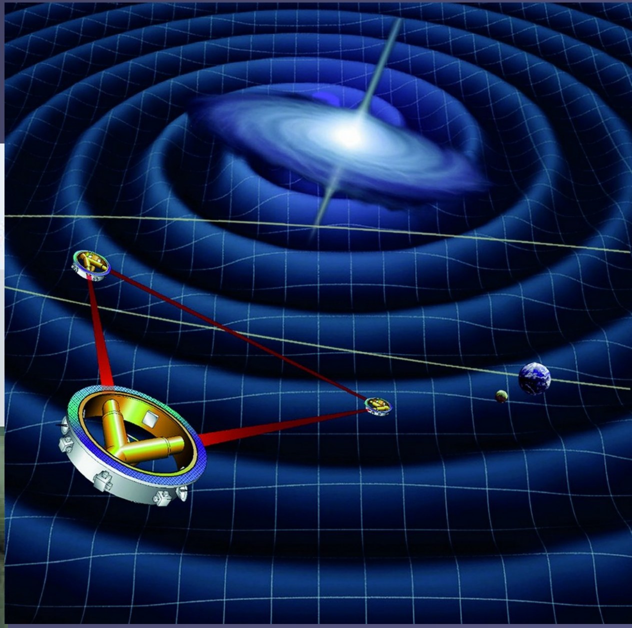

LISA =
Laser Space
Interferometer Antenna

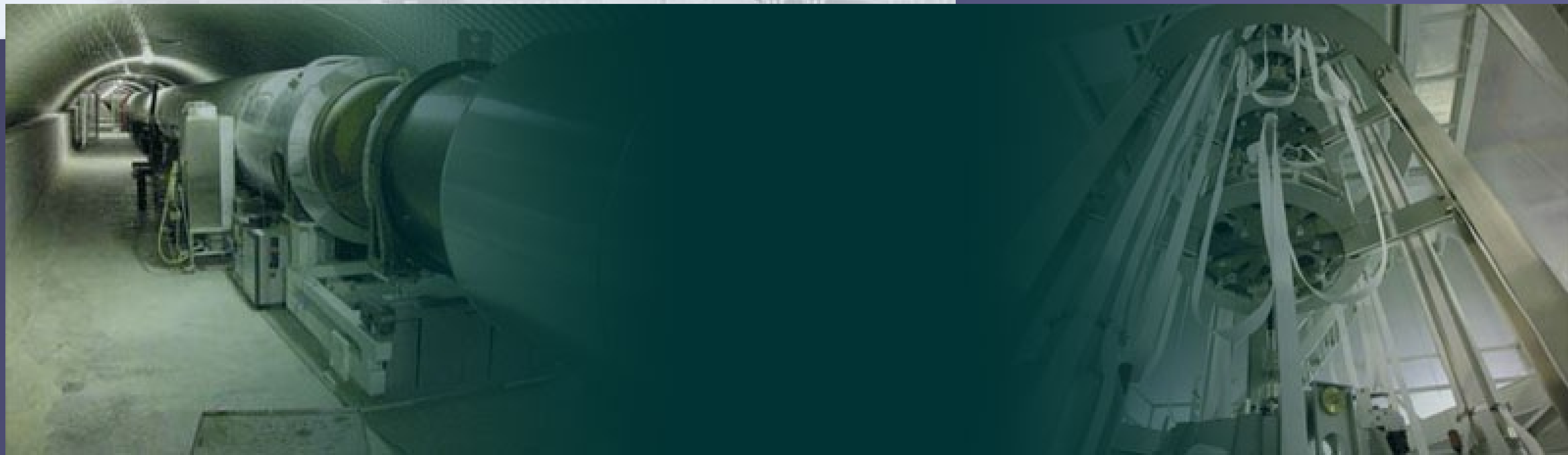

VIRGO – Pisa 3km
LIGO – Livingston, LA
Hanford, WA
4km
GEO600 – Hannover
600m
KAGRA - Japan

http://www.ligo-la.caltech.edu/
http://www.ego-gw.it
http://www.geo600.uni-hannover.de

Advanced:
Outreach to 50 Millionen light years (Neutron Stars)


Underground Gravitational Wave Detector —LCGT —
Kazuaki Kuroda
On behalf of LCGT

Now: KAGRA

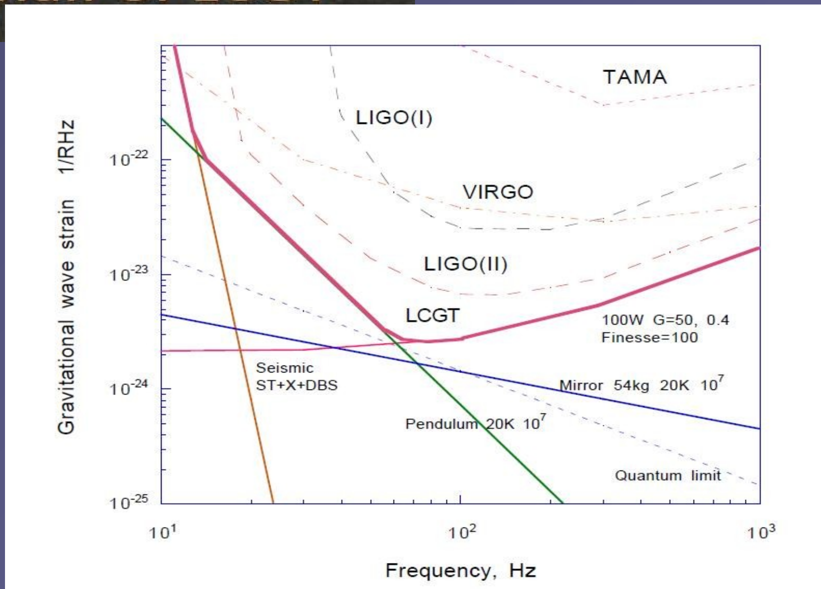
TAMA
LIGO(I)
VIRGO
LIGO(II)
LCGT
100W G=50, 0.4
Finesse=100
Seismic
ST+X+DBS
Mirror 54kg 20K 10^7
Pendulum 20K 10^7
Quantum limit
Gravitational wave strain 1/RHz
Frequency, Hz

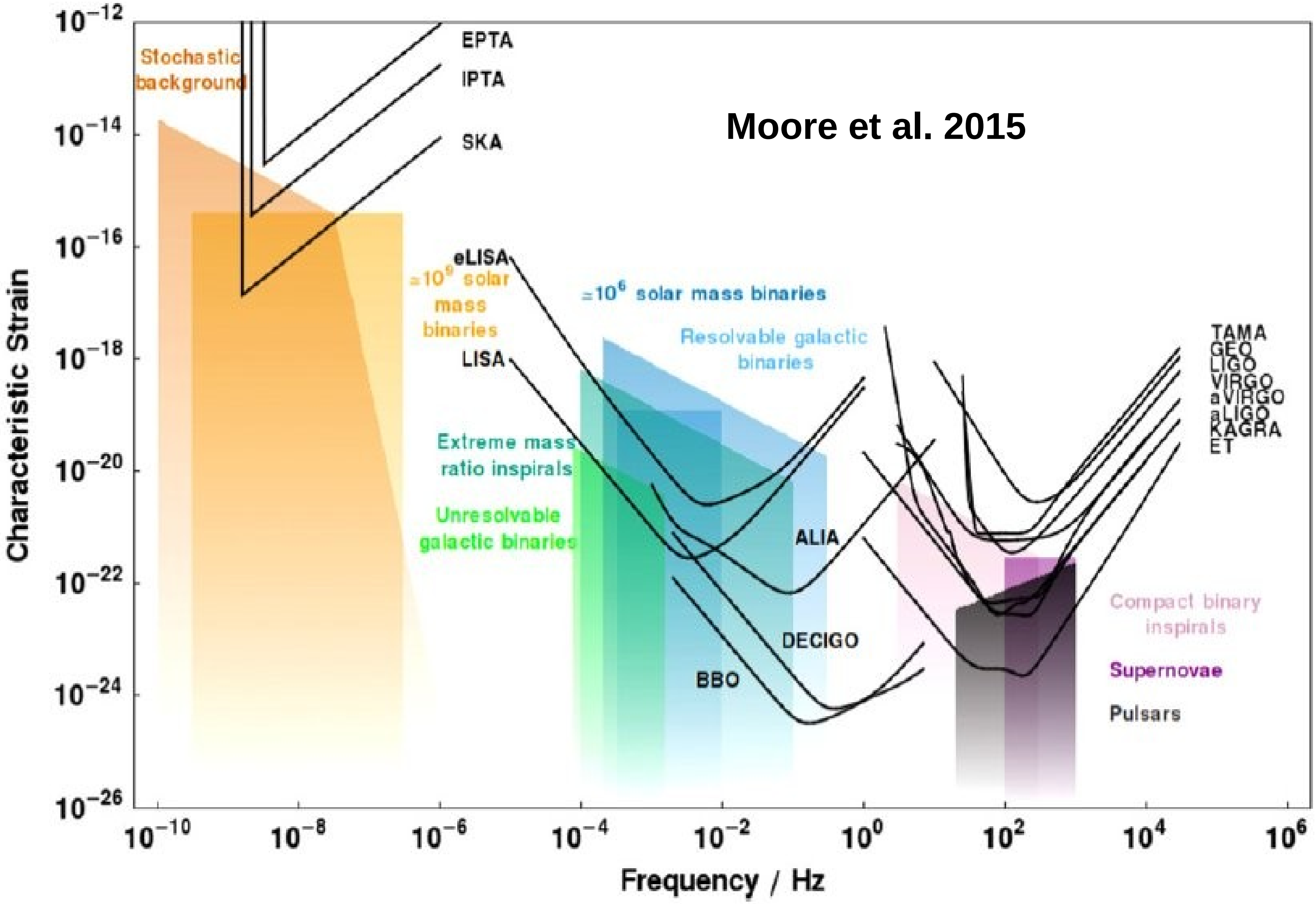

Figure A1. A plot of characteristic strain against frequency for a variety of detectors and sources.

1) Introduction – History

2) Star Cluster Dynamics with Black Holes and Gravitational Waves

1) <u>Star Clusters with IMBH formation</u>

2) Code(s) and Hardware

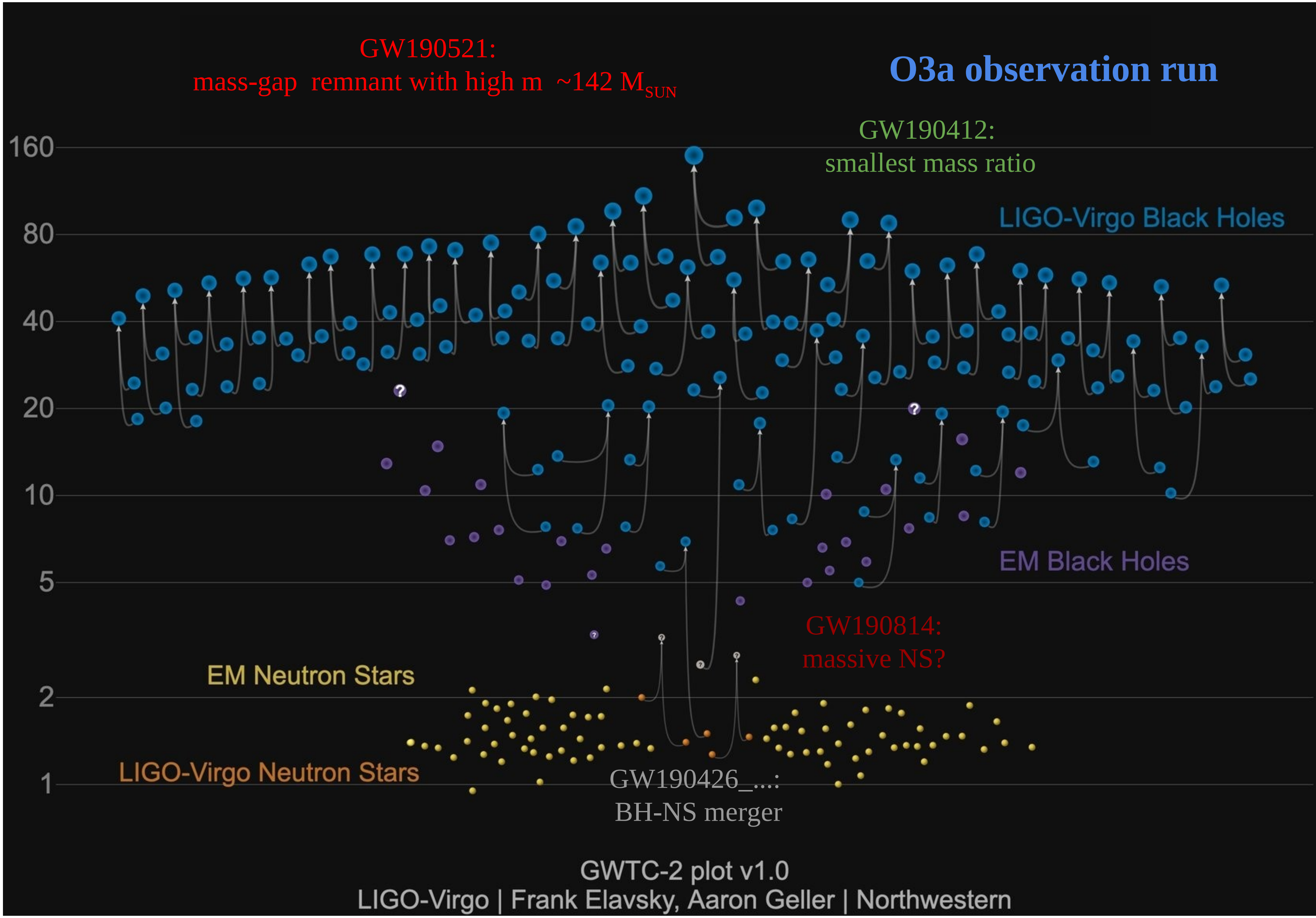
GW190521:
mass-gap remnant with high m ~142 M_SUN
O3a observation run
GW190412:
smallest mass ratio
LIGO-Virgo Black Holes
EM Black Holes
GW190814:
massive NS?
EM Neutron Stars
LIGO-Virgo Neutron Stars
GW190426_...:
BH-NS merger
160
80
40
20
10
5
2
1
GWTC-2 plot v1.0
LIGO-Virgo | Frank Elavsky, Aaron Geller | Northwestern

Mergers in the upper mass-gap: GW190521 and IMBHs

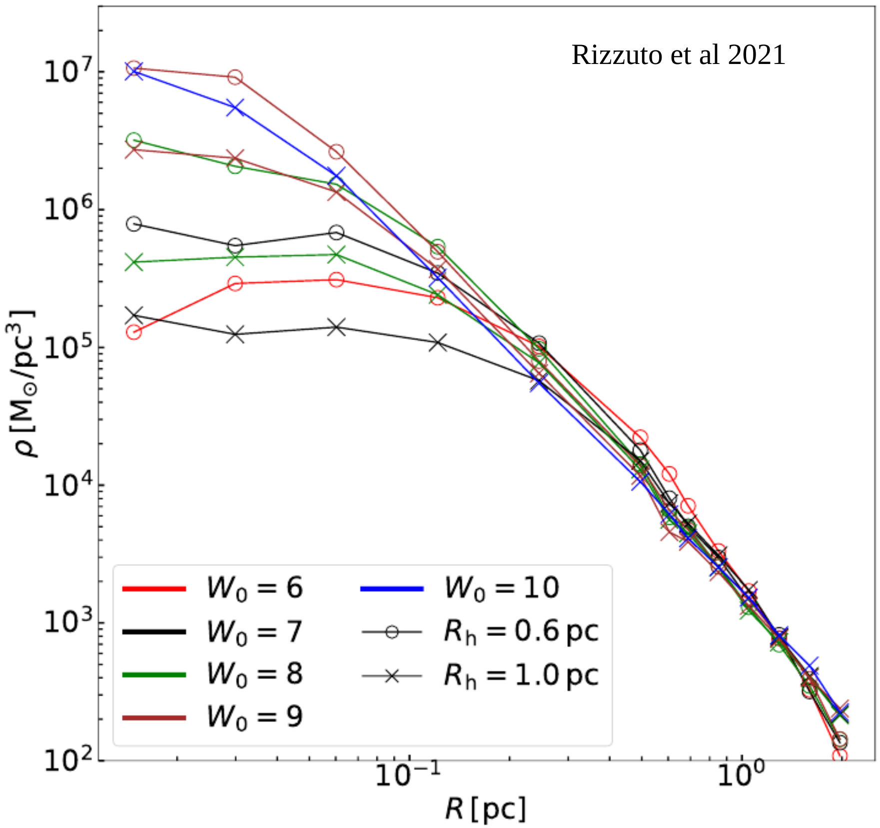

From Rizzuto et al (2021)

1. Direct *N*-body simulations using NBODY6++GPU improved: PN corrections but no GW recoil!
2. 80 simulations with

   N = 110k stars (10% binaries)

   $m_* = 0.08 - 100\ M_{SUN}$

1. Central density → $W_0 = 6 - 10$, $R_h = 0.6 - 1$ pc
2. Simulated time = 300 - 500 Myr
3. An IMBH forms in 17 cases (out of 80) with a mass > 100 M_{SUN}

From Arca Sedda et al (in prep)

1. Extract from the 80 models
   a. A handful of IMBH-BH mergers
   b. A fourth generation BH merger remnant
2. Use numerical relativity fitting formulae to
   a. Study the properties of remnants (mass, spin)
   – Assess the impact of GW kicks

Rizzuto et al (2021), MNRAS, 501, pp 5257-5273
Arca Sedda, M. et al, to be subm. to ApJ letters

Mergers in the upper mass-gap: GW190521 and IMBHs

Our IMBHs are the byproduct of a swift sequence of stellar collisions that build-up a very massive star that is accreted by a stellar BH.

Primary:

14 MS mergers +
3 MS mergers +
VMS-BH accretion =

VMS mass ~ 315 M_{SUN}

Secondary:

"Normal" stellar BH with mass 20 M_{SUN}

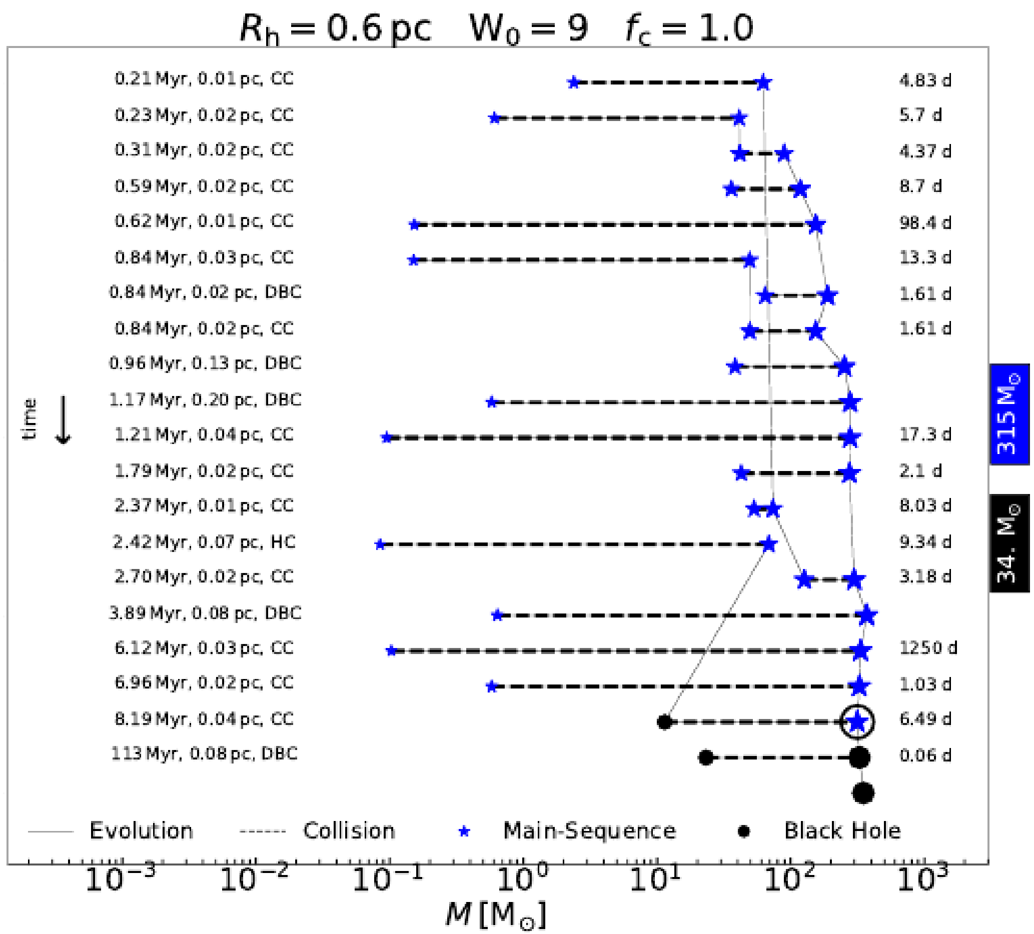

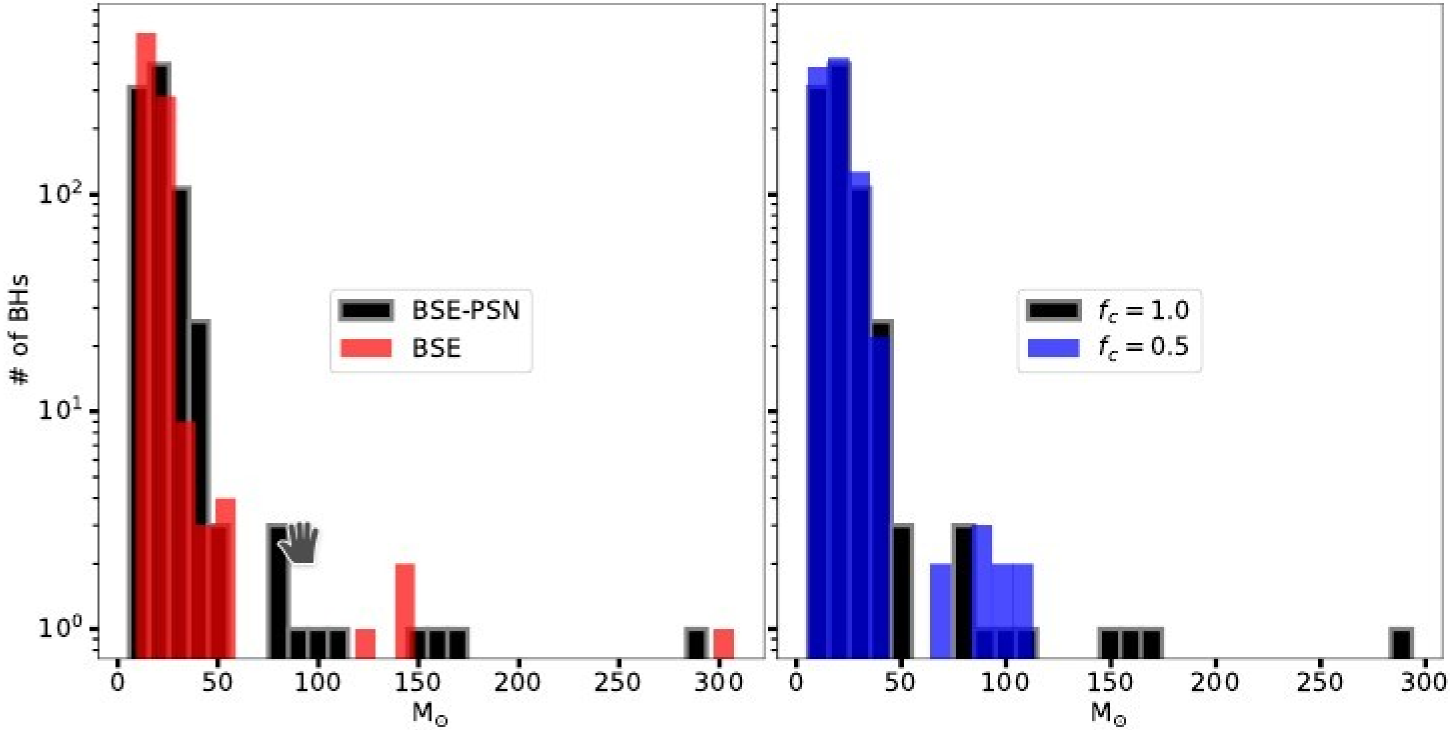

Figure 6. *Left panel:* Mass distribution of all BHs formed in the BSE model (red) and the BSE-PSN model (black) with $f_c = 1.0$ after 100 Myr of evolution. Simulations with BSE-PSN form more and more massive BHs in the (P)PSN mass gap and the IMBH mass regime. *Right panel:* Comparison of the BH mass distribution of the BSE-PSN model with $f_c = 1.0$ (black, same as left panel) to the model with $f_c = 0.5$ (blue). Lower accretion fractions for star-BH collisions result in less massive BHs.

Rizzuto, Naab, Spurzem, … Berczik, Arca Sedda, et al. 2022

Massive black hole formation in compact star clusters 13

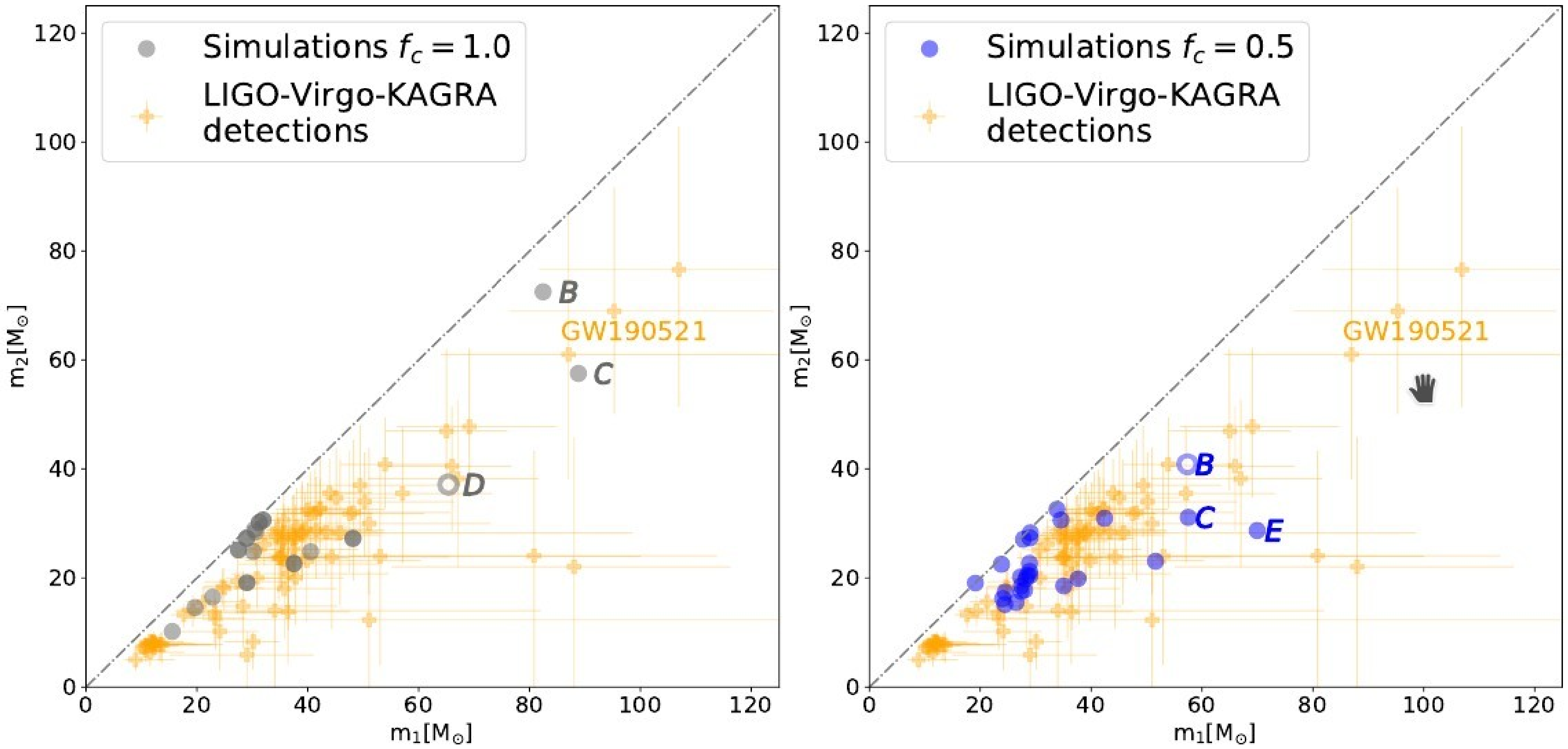

Rizzuto, Naab, Spurzem, Arca Sedda, Giersz, Banerjee, 2022

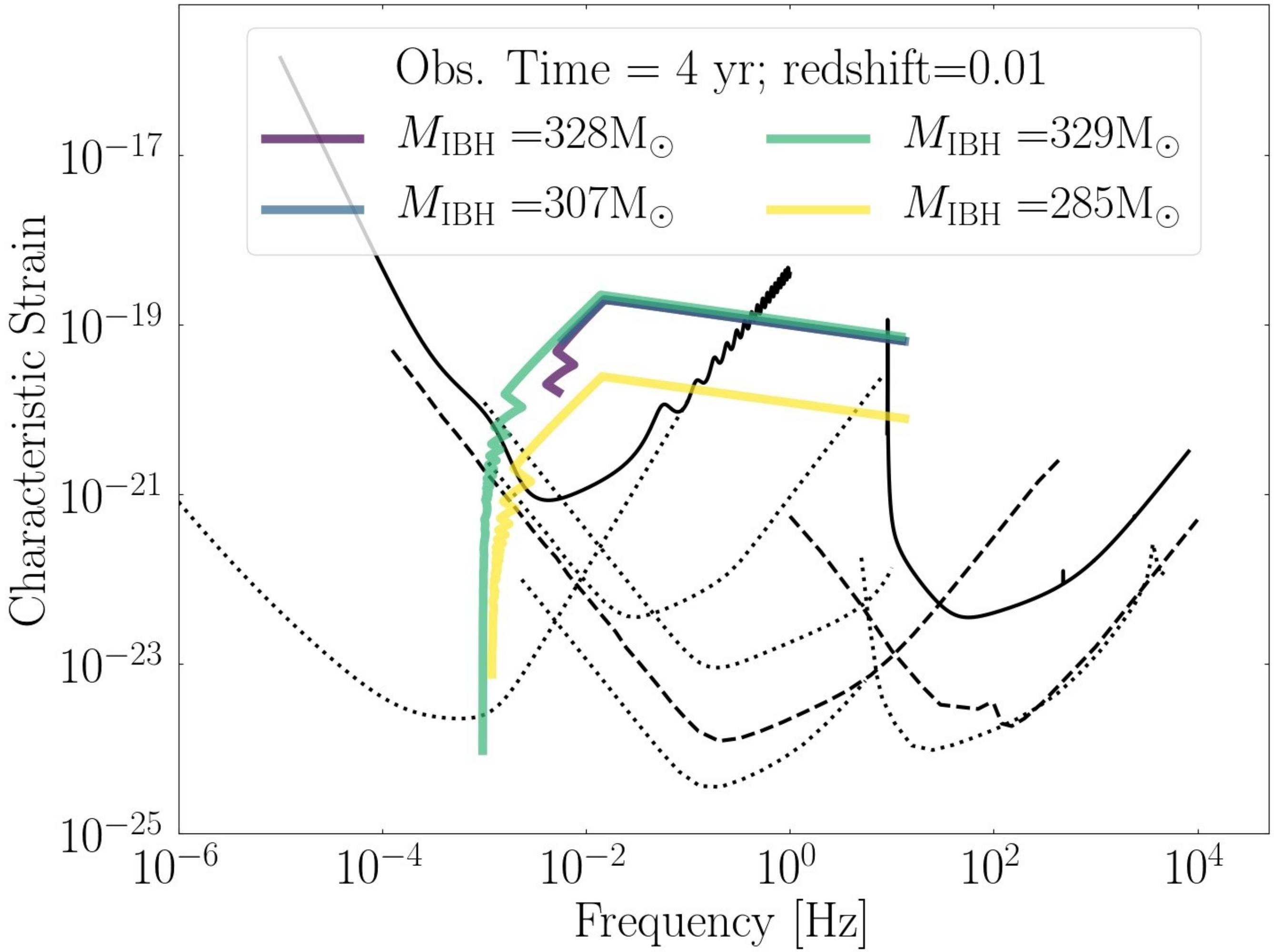

Arca Sedda, M. et al, to be subm. to ApJ letters

Rodriguez, Chatterjee, Rasio 2016: CMC (Monte Carlo Models) – approximate…
(compare also work of Giersz, Arca Sedda, Askar … MOCCA models)
(Many simulation models, but highly approximate...)

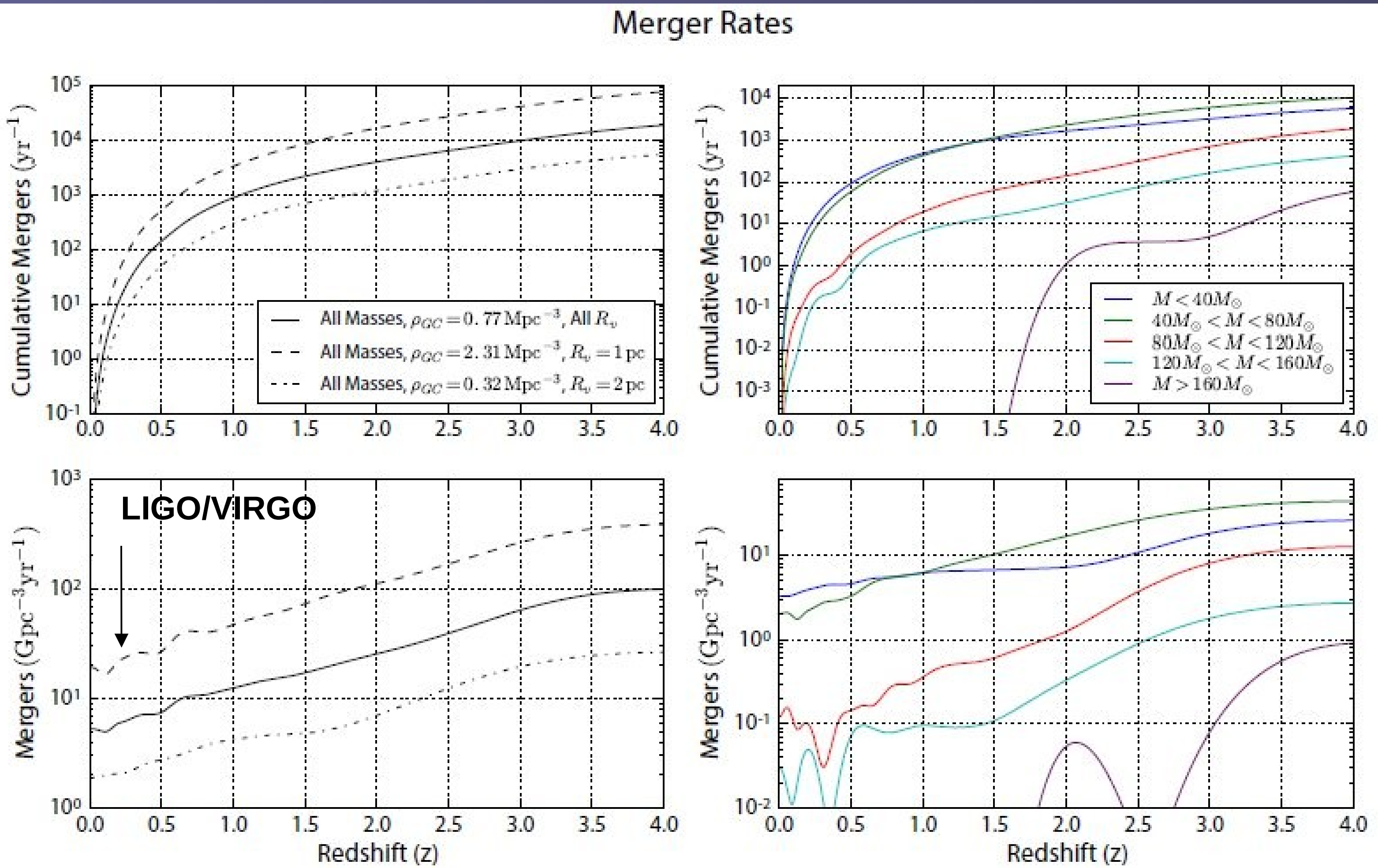

FIG. 12. The BBH merger rates from our models as a function of redshift. The upper panels show the cumulative rate of mergers per year in a volume out to redshift z, with the left panel showing the cumulative merger rate for all binaries, and the right panel showing the cumulative merger rate for binaries with specific total masses. The lower panels show the source merger rate in $\mathrm{Gpc}^{-3}\mathrm{yr}^{-1}$ at a given redshift for all BBHs (left) and for specific BBH total masses (right). For the total merger rates (the leftmost panels) we illustrate the uncertainties in our models to specific assumptions, showing how the rate varies with the spatial density of GCs and our choice of initial virial radius.

Black Holes were retained in globular clusters:

- **Before Strader et al. detection**
- **Before Breen & Heggie**
- **Before LIGO detection**

Downing 2012, Downing, Benacquista, Giersz & Spurzem, 2010, 2011:
(see also Banerjee, Baumgardt & Kroupa 2010 but …)

Compact Binaries in Star Clusters I - Black Hole Binaries Inside Globular Clusters

J. M. B. Downing[3*], M. Benacquista[4], R. Spurzem[1,2,3], and M. Giersz[5]
[1] *National Astronomical Observatories, Chinese Academy of Sciences, 20A Datun Ln, Chaoyang District, 100012, China*
[2] *Kavli Institute of Astronomy and Astrophysics, Peking University, Beijing, China*
[3] *Astronomisches Rechen-Institut, Zentrum für Astronomie der Universität Heidelberg, Monchhofsraβe 12-14, D-69120 Heidelberg, Germany*
[4] *Center for Gravitational Wave Astronomy, University of Texas at Brownsville, Brownsville, TX 78520, USA*
[5] *Nicolaus Copernicus Astronomical Center, Polish Academy of Sciences, ul. Bartycka 18, 00-716 Warsaw, Poland*

Compact Binaries in Star Clusters II - Escapers and Detection Rates

J. M. B. Downing[1,2*], M. J. Benacquista[3], M. Giersz[4], and R. Spurzem[5,6,1]
[1] *Astronomisches Rechen-Institut, Zentrum für Astronomie der Universität Heidelberg, Monchhofsraβe 12-14, D-69120 Heidelberg, Germany*
[2] *Fellow of the International Max-Planck Research School for Astronomy and Cosmic Physics at the University of Heidelberg, Heidelberg, Germany*
[3] *Center for Gravitational Wave Astronomy, University of Texas at Brownsville, Brownsville, TX 78520, USA*
[4] *Nicolaus Copernicus Astronomical Center, Polish Academy of Sciences, ul. Bartycka 18, 00-716 Warsaw, Poland*
[5] *National Astronomical Observatories, Chinese Academy of Sciences, 20A Datun Rd., Chaoyang District, 100012, China*
[6] *Kavli Institute of Astronomy and Astrophysics, Peking University, Beijing, China*

Is there a size difference between red and blue globular clusters?

J. M. B. Downing[*]
Astronomisches Rechen-Institue, Zentrum für Astronomie der Universität Heidelberg, Mönchhofstraβe 12-14, D-69120 Heidelberg, Germany

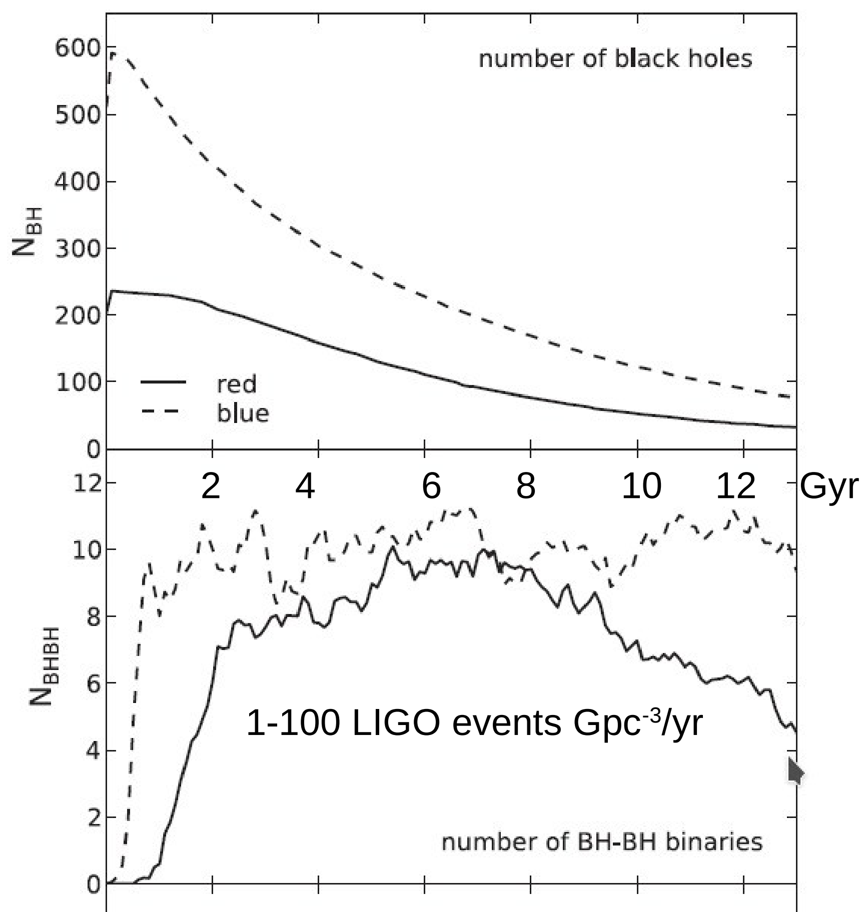

Globular clusters: NGC 3201

NGC 3201 (Orion Optics UK AG12Orion telescope): http://www.astro-austral.cl/imagenes/st

- Globular clusters (GCs) are extremely old → fossil remnants of early galaxy formation
- Milky Way hosts over 150 of these
- GCs are extremely dense
- Host hierarchical stellar systems, especially in their cores that act as a kind of heat source → delay core-collapse

NGC 3201

Slide by A. Kamlah Figure: Giesers et al. 2019

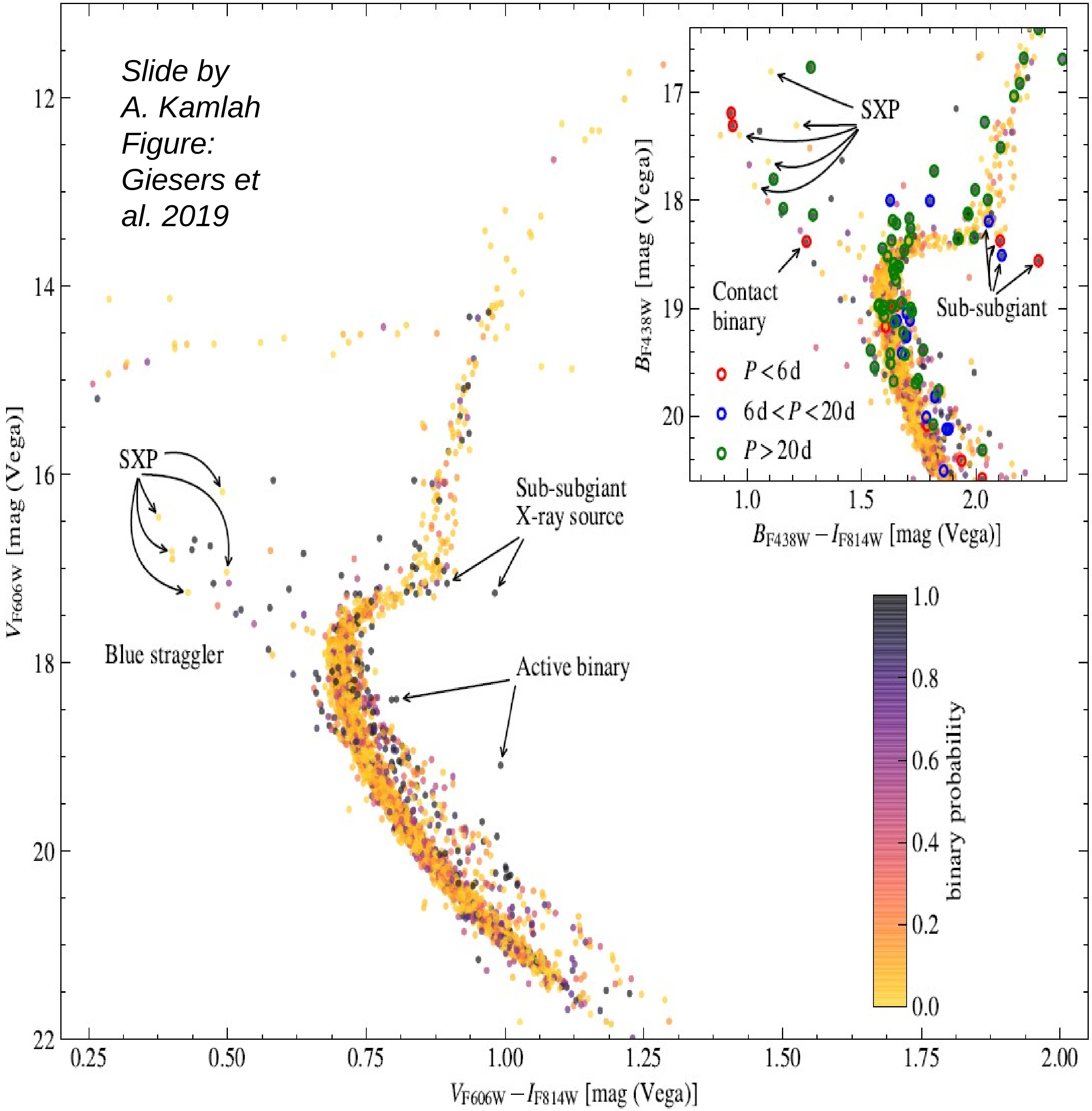

- Very old and metal-poor GC
- Negligbly rotating today (Bianchini et al. 2018) → initially rotating much faster?
- Large half mass radius of 6.20 pc → BH subsystem / hard binary subsystem that counters core-collapse?
- Three stellar mass BH binaries found in MUSE data (Giesers et al. 2018, 2019)

→ DRAGON-II NGC 3201 simulation project

Figure: Giesers et al. 2019; HST survey: Nardiello et al. 2018; Piotto et al. 2015; See also Askar et al. 2018; Kremer et al. 2018 Giesers et al. 2018; Price-Whelan et al. 2018

1) Introduction – History
2) Star Cluster Dynamics with Black Holes and Gravitational Waves
1) Star Clusters with IMBH formation
2) **Code(s) and Hardware**

Computational Science...

...after von Neumann...

Exaflop/s?

Petaflop/s

Teraflop/s

Gigaflop/s

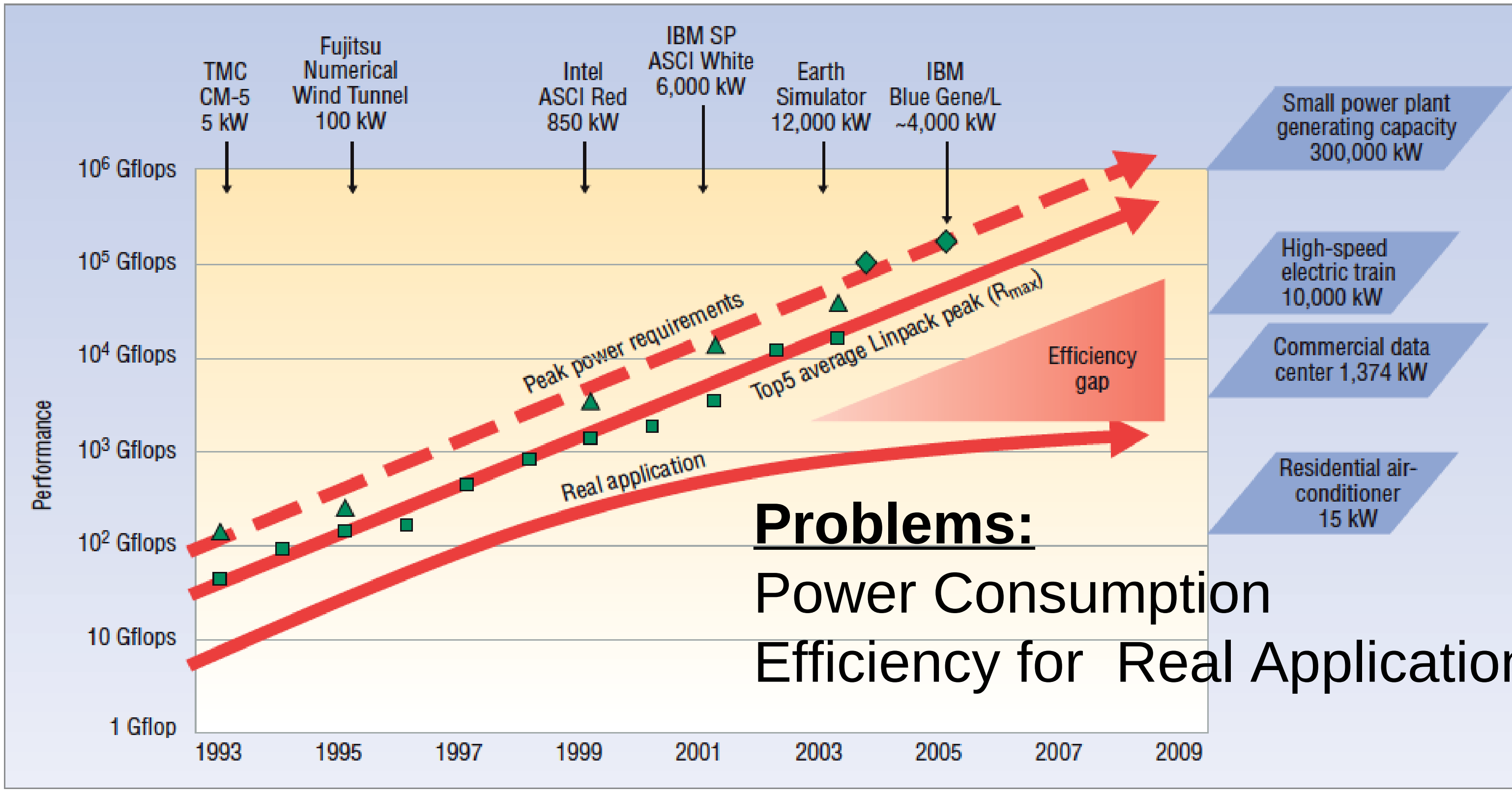

Problems:

Power Consumption

Efficiency for Real Applications

Figure 1. Rising power requirements. Peak power consumption of the top supercomputers has steadily increased over the past 15 years.

Thanks to Horst Simon, LBNL/NERSC for this diagram.

HARDWARE

GRAPE-6 Gravity/Coulomb Part

- G6 Chip: 0.25μ 2MGate ASIC, 6 Pipelines
- at 90MHz, 31Gflops/chip
- 48Tflops full system (March 2002)
- Plan up to 72Tflops full system (in 2002)
- Installed in Cambridge, Marseille, Drexel, Amsterdam, New York (AMNH), Mitaka (NAO), Tokyo, etc..
  New Jersey, Indiana, Heidelberg

NAOC laohu cluster

64 Kepler K20

Laohu: 2009/2015
(Kepler GPU)
100 Tflop/s 150k cores

New GPUs 5-6 times faster… (see below)

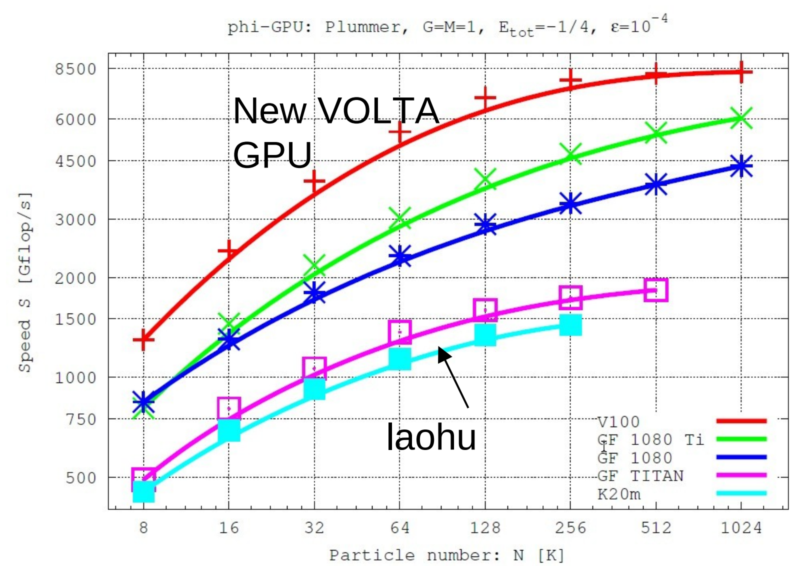

GPU Clusters used:

<u>JUWELS Booster GPU Partition (Ampere A100 GPU)</u>

Golowood cluster, Main Astron. Observatory, Kiev, Ukraine

Kepler/bwFor clusters Heidelberg, Germany (12x +18x Kepler GPU)

Max-Planck MPCDF GPU clusters

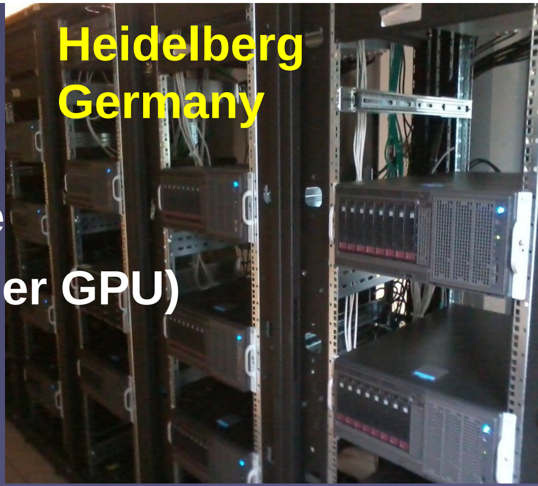

PRACE

PRACE Award - 2011

Astrophysical Particle Simulations with Large Custom GPU Clusters on Three Continents

Rainer Spurzem, *et al*, Chinese Academy of Sciences & University of Heidelberg

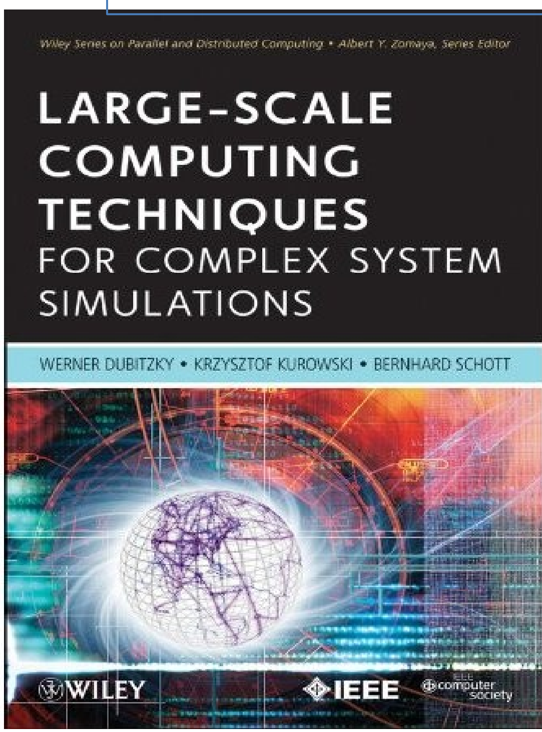

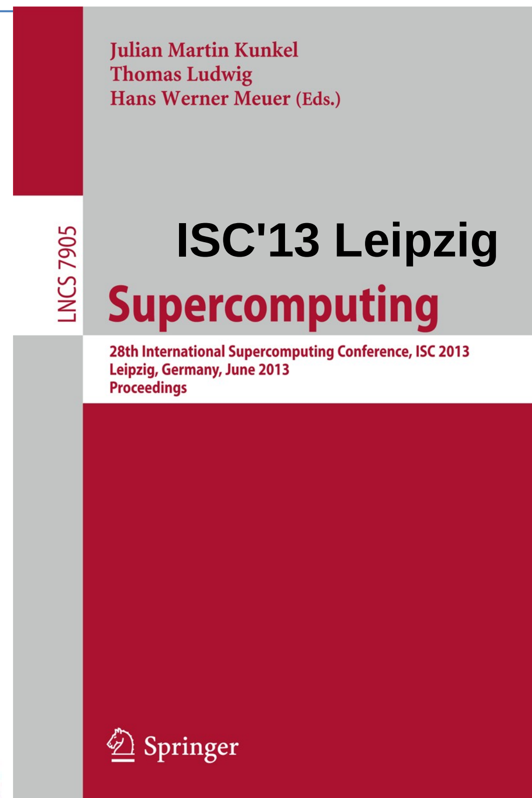

NAOC 中国科学院国家天文台 NATIONAL ASTRONOMICAL OBSERVATORIES ,CHINESE ACADEMY OF SCIENCES

北京大學 PEKING UNIVERSITY

Physical and Numerical Methods: Direct Simulations
Direct: high accuracy / active-inactive particles

The Hermite Scheme: 4th Order on two time points

$$\vec{a}_0 = \sum_j G m_j \frac{\vec{R}_j}{R_j^3} \quad ; \quad \dot{\vec{a}}_0 = \sum_j G m_j \left[\frac{\vec{V}_j}{R_j^3} - \frac{3(\vec{V}_j \cdot \vec{R}_j)\vec{R}_j}{R_j^5} \right] ,$$

$$\vec{x}_p(t) = \frac{1}{6}(t-t_0)^3 \dot{\vec{a}}_0 + \frac{1}{2}(t-t_0)^2 \vec{a}_0 + (t-t_0)\vec{v} + \vec{x} ,$$
$$\vec{v}_p(t) = \frac{1}{2}(t-t_0)^2 \dot{\vec{a}}_0 + (t-t_0)\vec{a}_0 + \vec{v} ,$$

Repeat Step 1 at t_1 using predicted x,v → $a_{1,}$ $å_1$

Physical and Numerical Methods: Direct Simulations

$$\frac{1}{2}\vec{a}^{(2)} = -3\frac{\vec{a}_0 - \vec{a}_1}{(t-t_0)^2} - \frac{2\dot{\vec{a}}_0 + \dot{\vec{a}}_1}{(t-t_0)}$$

$$\frac{1}{6}\vec{a}^{(3)} = 2\frac{\vec{a}_0 - \vec{a}_1}{(t-t_0)^3} - \frac{\dot{\vec{a}}_0 + \dot{\vec{a}}_1}{(t-t_0)^2} ,$$

The Hermite Step

Get Higher Derivatives

$$\vec{x}(t) = \vec{x}_p(t) + \frac{1}{24}(t-t_0)^4\vec{a}_0^{(2)} + \frac{1}{120}(t-t_0)^5\vec{a}^{(3)} ,$$

$$\vec{v}(t) = \vec{v}_p(t) + \frac{1}{6}(t-t_0)^3\vec{a}_0^{(2)} + \frac{1}{24}(t-t_0)^4\vec{a}_0^{(3)} .$$

The Corrector Step – this is not time symmetric!

Physical and Numerical Methods: Direct Simulations

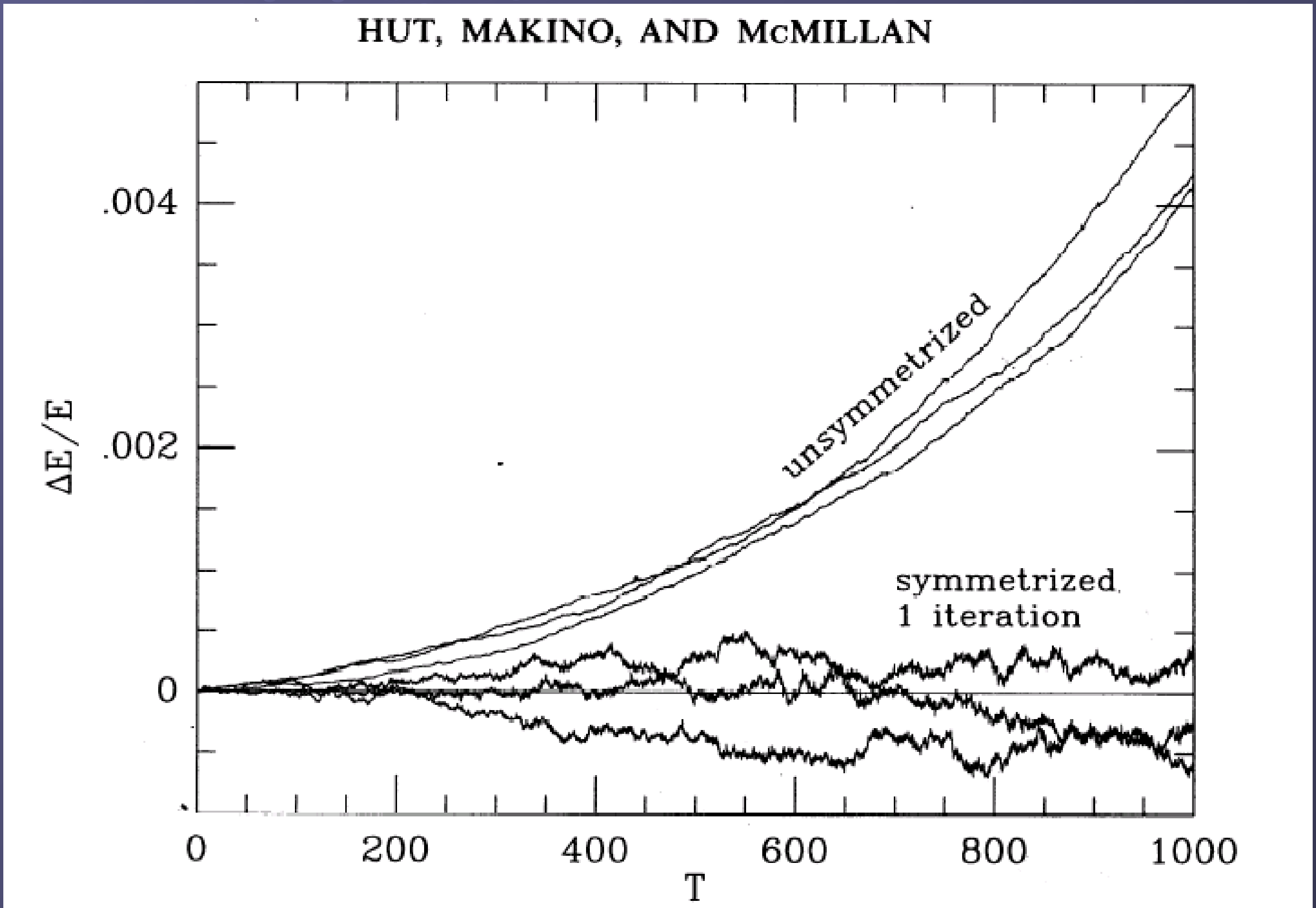

1995

N=100

1000 orb.times

Acronym	Algorithm	Scaling	Comments
PM	Particle Mesh	$N\ n_c^3 \log_2 n_c^3$ (1)	fixed geometry
FMP	Fast Multipole	$N\ nlm$	req. equal Δt
SCF	Self-Consistent Field	$N\ nlm$	series evaluation (2)
NBODY1	Aarseth	N^2	ITS, softening
NBODY1++	Hermite	N^2	HTS, softening
NBODY2	Aarseth, AC	$NN_n + N^2/\gamma$	ITS, softening, (3)
NBODY3	Aarseth	N^2	ITS, KS-reg.
NBODY4	Hermite	N^2	HTS, KS-reg.
NBODY5	Aarseth, AC	$NN_n + N^2/\gamma$	ITS, KS-reg., (3)
NBODY6	Hermite, AC	$NN_n + N^2/\gamma$	HTS, KS-reg., (3)
NBODY6++/GPU	parallel NBODY6	$NN_n + N^2/\gamma$	HTS, KS-reg., (3,4)
KIRA	Hermite	N^2	HTS, (5)
TREE	TREE-code	$N \ln N$	N^2 for high accuracy
P^{3}M	Part.-Part. PM	$N_n^2\ n_c^3 \log_2 n_c^3$ (1)	fixed geometry (6)

softening: singularity in pairwise potential removed by softening parameter ε
ITS: Individual Time Step Scheme
HTS: Hierarchical Block Time Step Scheme
KS-reg.: KS regularization of perturbed two- and hierarchical N-body motion [48,68]
AC: Ahmad-Cohen neighbour scheme [5]
(1) Discrete FFT on regular 3D mesh with n linear mesh points assumed
(2) Sufficient Accuracy requires appropriate basis function set [37]
(3) γ: ratio of regular to irregular time step
(4) speedup by parallel execution not contained in scaling, see [81]
(5) New high accuracy Hermite code based on STARLAB [64,75]
(6) with hierarchically nested adaptive grids used for cosmological simulations [73]

Physical and Numerical Methods:
Other Algorithms

gyrfalcon	fast multipole (Dehnen)
FROST	direct N-Body (Rantala)
PeTaR	N-Body-Tree (Wang)

(Spurzem 1999) + notes added

A brief comparison of the code versions:

ITS: Individual time–steps
ACS: Neighbour scheme (Ahmad–Cohen scheme) with block time–steps
KS: KS–regularization of few-body subsystems
HITS: Hermite scheme integration method combined with hierarchical block time steps
PN: Post-Newtonian terms
AR: Algorithmic regularization

	ITS	ACS	KS	HITS	PN	AR
NBODY1	✓					
NBODY2		✓		✓		
NBODY3	✓		✓			
NBODY4			✓	✓		
NBODY5	✓	✓	✓			
NBODY6		✓	✓	✓		
NBODY7		✓	✓	✓	✓	✓

NBODY6++ / NBODY6GPU / NBODY6++GPU

NBODY6++

Manual for the Computer Code

Emil Khalisi, Long Wang, Rainer Spurzem

Astronomisches Rechen–Institut

Mönchhofstr. 12–14, 69120 Heidelberg, Germany Kavli Institute for Astronomy and Astrophysics, Peking University, Beijing, China

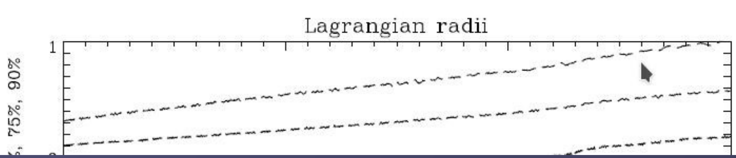

Ahmad-Cohen
Neighbour Scheme

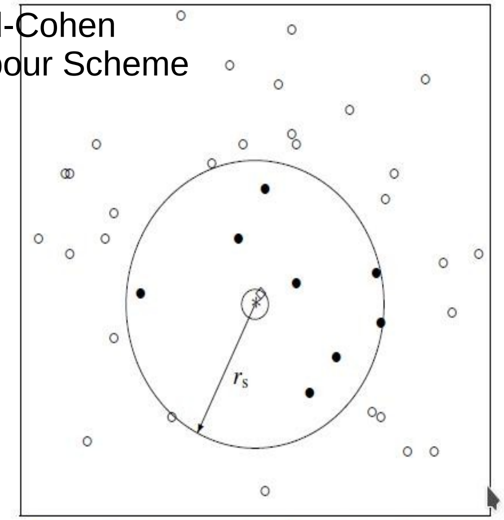

igure 10.1: Illustration of the neighbour scheme for particle *i* marked as the asterisk (after [2]).

Our own φGRAPE/GPU N-body code

~N

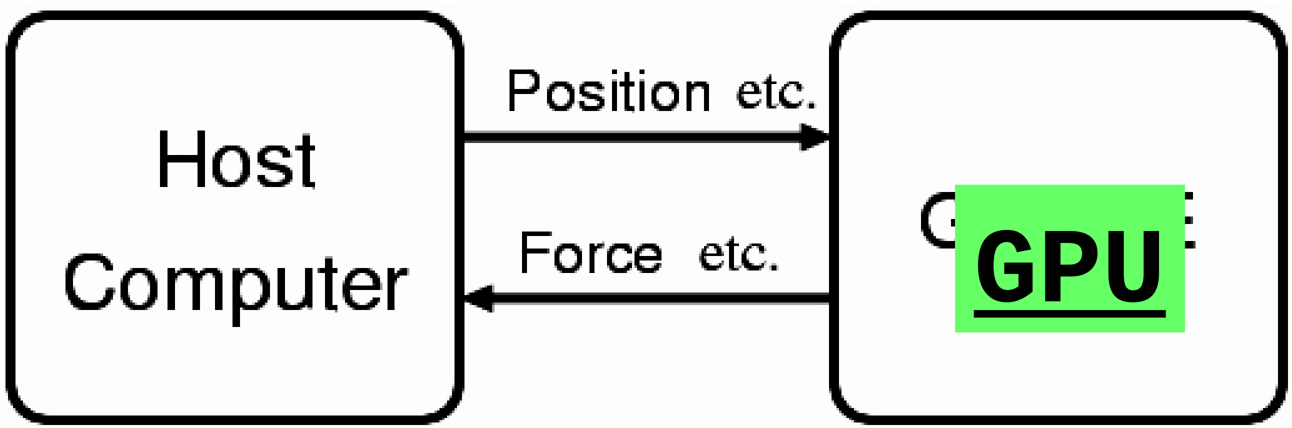

~N^2

$$\vec{a}_i = \sum_{j=1;j\neq i}^{N} \vec{f}_{ij} \quad \vec{f}_{ij} = -\frac{G \cdot m_j}{\left(r_{ij}^2 + \varepsilon^2\right)^{3/2}} \vec{r}_{ij}$$

Slide: Peter Berczik

Software

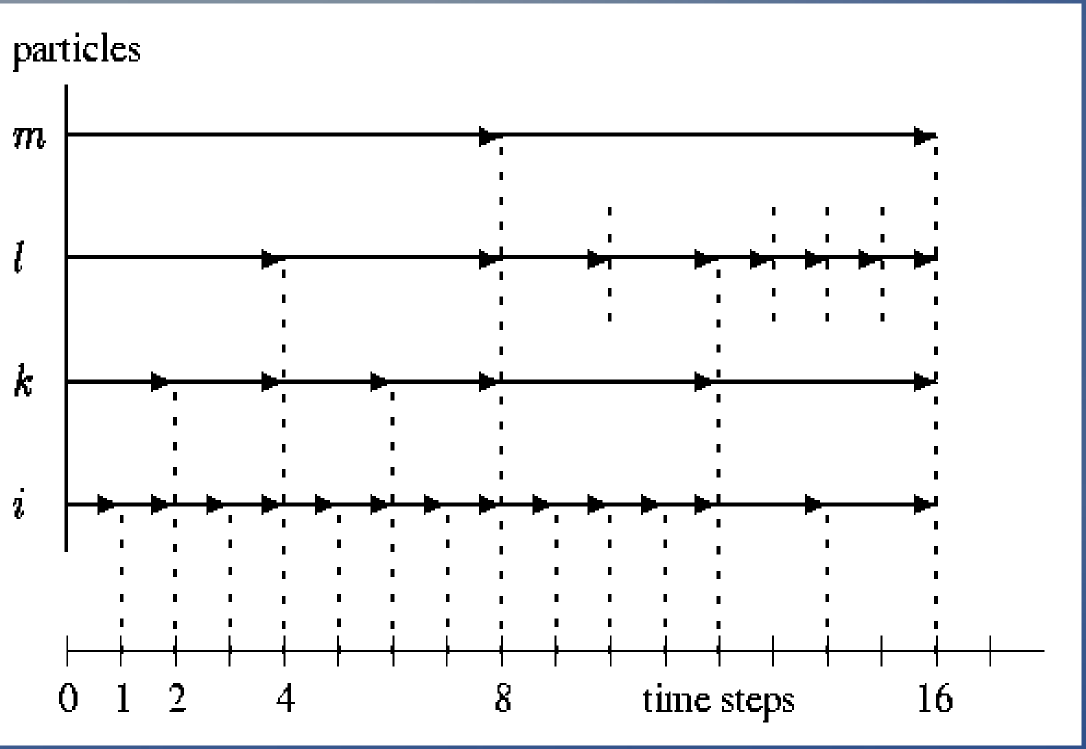

S.J.Aarseth, S. Mikkola
(ca. 20.000 lines):

- Hierarchical Block Time Steps
- Ahmad-Cohen Scheme
- Regularisations
- 4th order Hermite scheme

- NBODY6 (Aarseth 1999)
- NBODY6++ (Spurzem 1999) MPI
- NBODY6++GPU (Wang, Spurzem, Aarseth et al. 2015)

Hierarchical Block Time Steps

$$\Delta t = \sqrt{\eta \frac{|\vec{a}||\vec{a}^{(2)}| + |\dot{\vec{a}}|^2}{|\dot{\vec{a}}||\vec{a}^{(3)}| + |\vec{a}^{(2)}|^2}} \, .$$

Software

NBODY4, NBODY6, S.J.Aarseth, S. Mikkola, ...
(ca. 20.000 lines, since 1963):

- Hierarchical Individual Time Steps (HITS)
- Ahmad-Cohen Neighbour Scheme (ACS)
- Kustaanheimo-Stiefel and Chain-Regular. (KSREG) for bound subsystems of N<6 (Quaternions!)
- 4th order Hermite scheme (pred/corr), Bulirsch-Stoer (for Chain)
- Stellar Evolution (single/binary) (w Hurley)

- *NBODY6++GPU, φGPU, L. Wang, R. Spurzem, P. Berczik, K. Nitadori,...*
- *(massively parallel codes, since 1999, recent paper Wang, Spurzem, Aarseth, et al. 2015):*
- NBODY6++ (Spurzem 1999) using MPI
- Parallel φGRAPE / φGPU (Harfst et al. 2006, Spurzem et al. 2009)
- NBODY6++/GPU-MPI (Wang, Spurzem, Aarseth, et al. 2015)
- Parallel Binary Integration in Progress (KSREG)

Our CPU/GPU N-body (AC) code

NBODY6++GPU

Wang, Spurzem, Aarseth, et al. 2015, 2016
→ Exaflop/s Huang, Berczik, Spurzem 2016

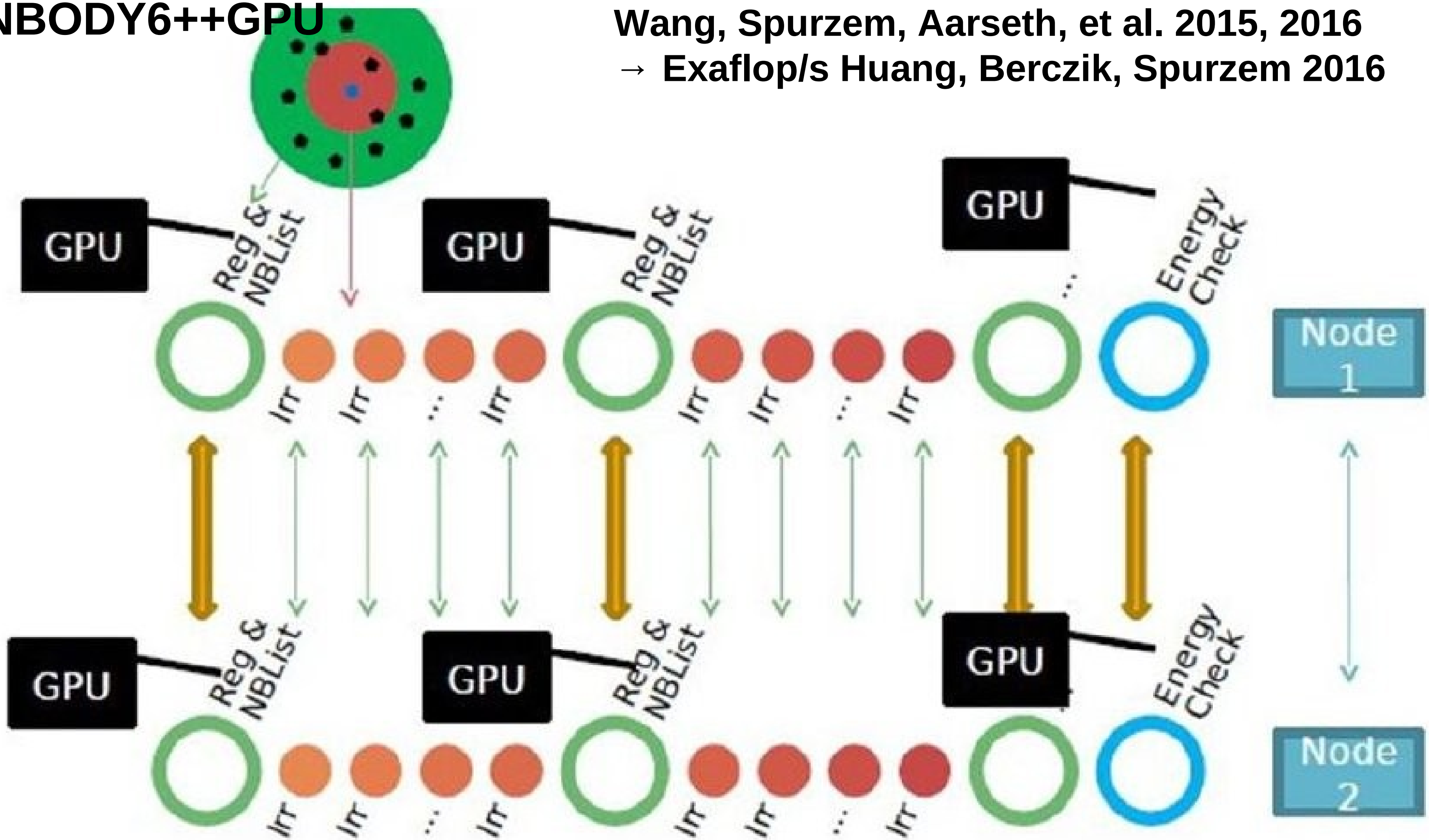

https://github.com/lwang-astro/betanb6pp

“Moore's” Law for Direct N-Body

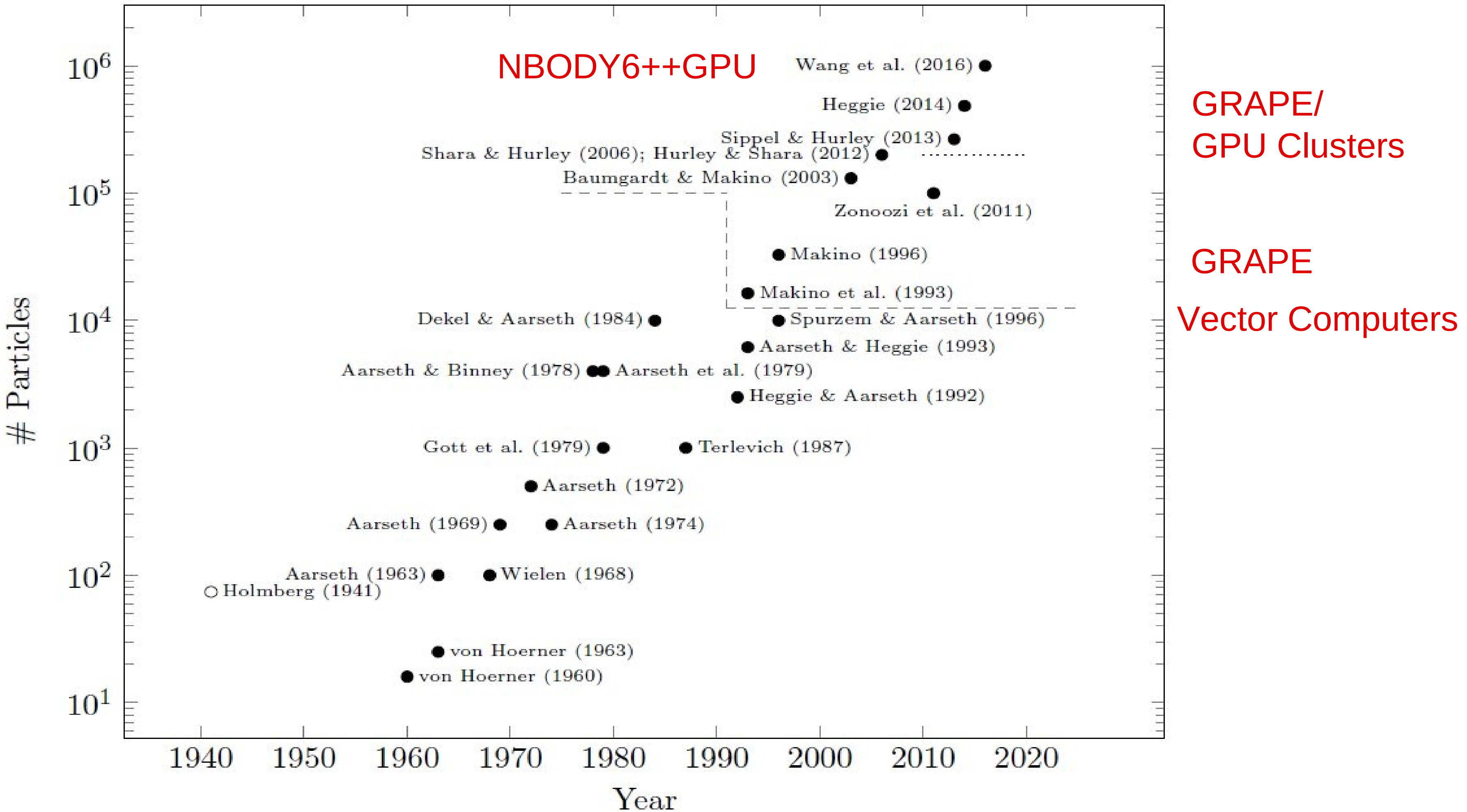

by D.C. Heggie with added new cits. Sippel

To demonstrate how successful the direct NBODY codes are in our field we have collected the following three figures from the ADS Bumblebee (full text search) facility. The search string

full:NBODY5 OR full:NBODY6 OR full:"NBODY6++" OR full:NBODY7 OR full:NBODY4

has been used to catch all publications using or citing the different variants of the code.

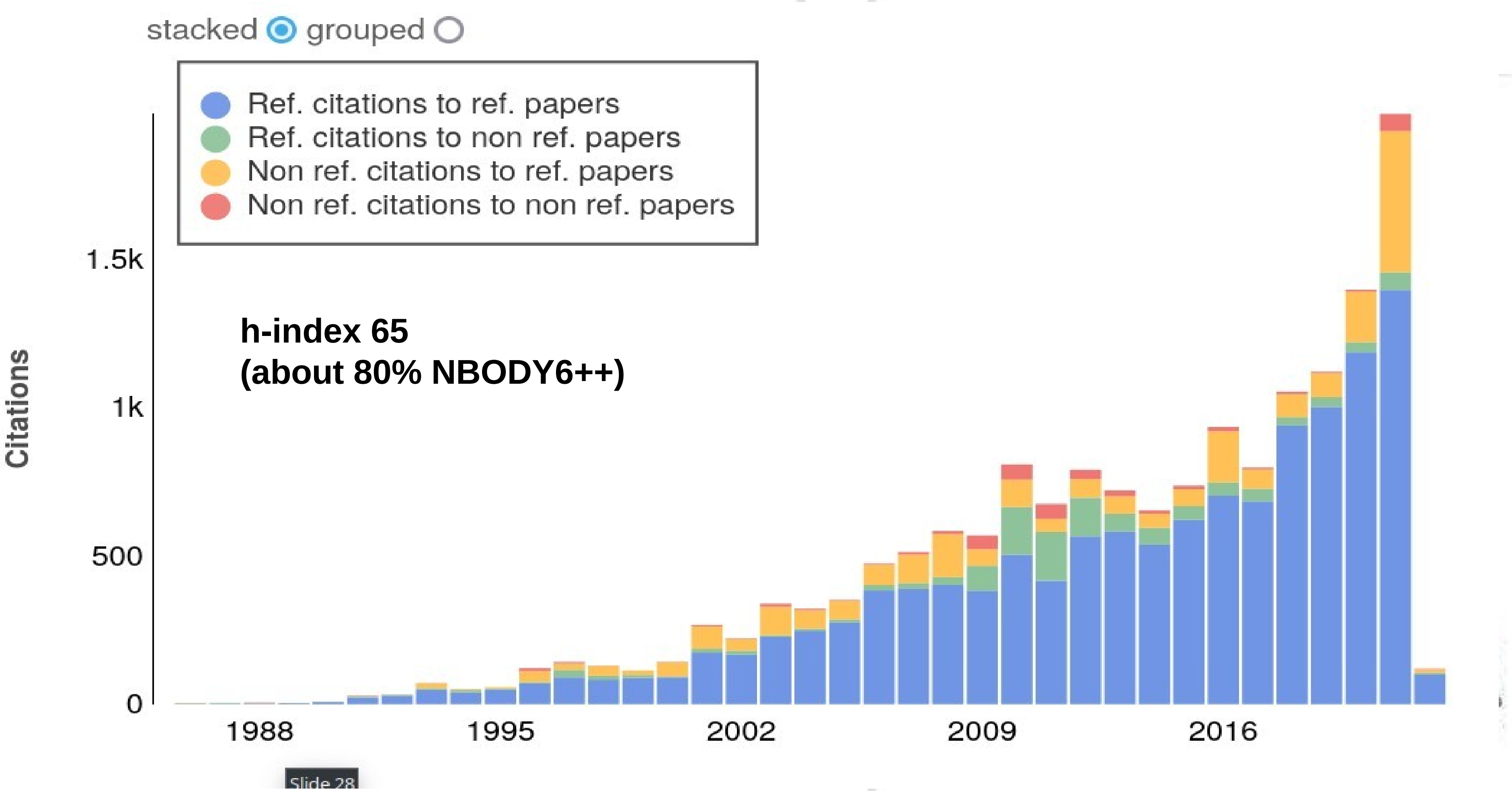

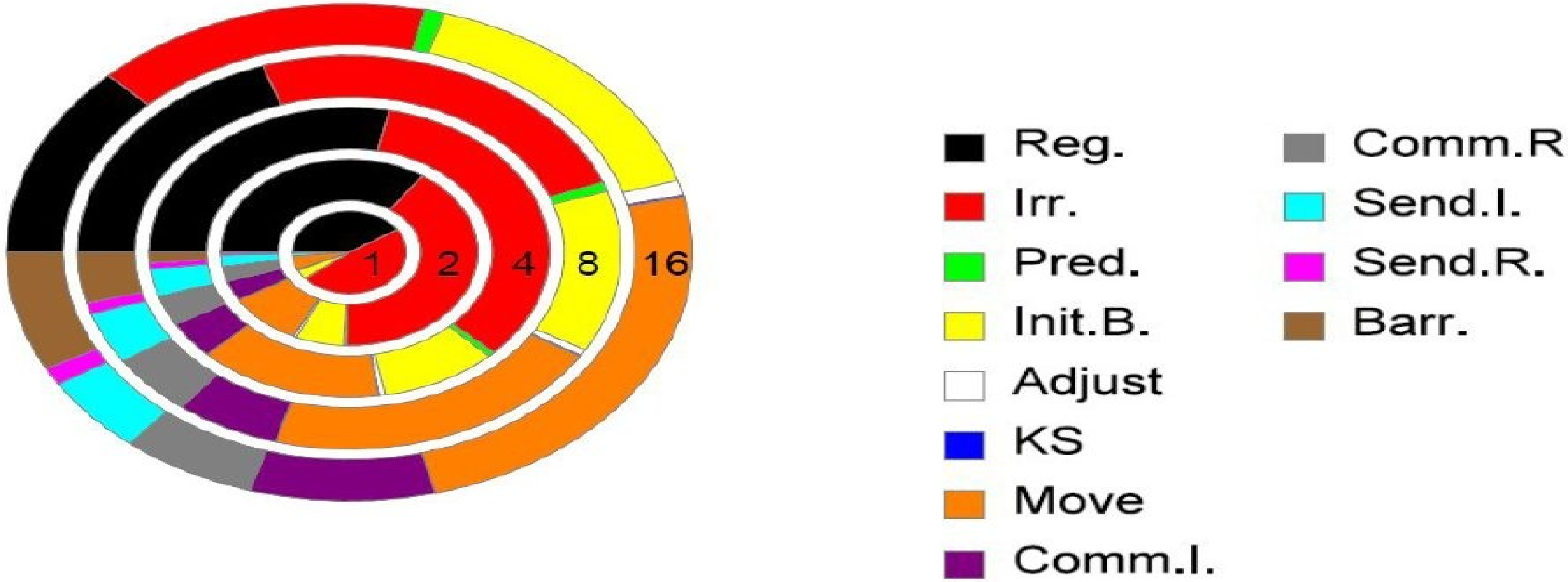

Table 1 Main components of NBODY6++

Description	Timing variable	Expected scaling N	Expected scaling N_p	Fitting value [sec]
Regular force computation	$T_{\rm reg}$	$\mathcal{O}(N_{\rm reg} \cdot N)$	$\mathcal{O}(N_p^{-1})$	$(2.2 \cdot 10^{-9} \cdot N^{2.11} + 10.43) \cdot N_p^{-1}$
Irregular force computation	$T_{\rm irr}$	$\mathcal{O}(N_{\rm irr} \cdot \langle N_{nb} \rangle)$	$\mathcal{O}(N_p^{-1})$	$(3.9 \cdot 10^{-7} \cdot N^{1.76} - 16.47) \cdot N_p^{-1}$
Prediction	$T_{\rm pre}$	$\mathcal{O}(N^{kn_p})$	$\mathcal{O}(N_p^{-kp_p})$	$(1.2 \cdot 10^{-6} \cdot N^{1.51} - 3.58) \cdot N_p^{-0.5}$
Data moving	$T_{\rm mov}$	$\mathcal{O}(N^{kn_{m1}})$	$\mathcal{O}(1)$	$2.5 \cdot 10^{-6} \cdot N^{1.29} - 0.28$
MPI communication (regular)	$T_{\rm mcr}$	$\mathcal{O}(N^{kn_{cr}})$	$\mathcal{O}(kp_{cr} \cdot \frac{N_p-1}{N_p})$	$(3.3 \cdot 10^{-6} \cdot N^{1.18} + 0.12)(1.5 \cdot \frac{N_p-1}{N_p})$
MPI communication (irregular)	$T_{\rm mci}$	$\mathcal{O}(N^{kn_{ci}})$	$\mathcal{O}(kp_{ci} \cdot \frac{N_p-1}{N_p})$	$(3.6 \cdot 10^{-7} \cdot N^{1.40} + 0.56)(1.5 \cdot \frac{N_p-1}{N_p})$
Synchronization	$T_{\rm syn}$	$\mathcal{O}(N^{kn_s})$	$\mathcal{O}(N_p^{kp_s})$	$(4.1 \cdot 10^{-8} \cdot N^{1.34} + 0.07) \cdot N_p$
Sequential parts on host	$T_{\rm host}$	$\mathcal{O}(N^{kn_h})$	$\mathcal{O}(1)$	$4.4 \cdot 10^{-7} \cdot N^{1.49} + 1.23$

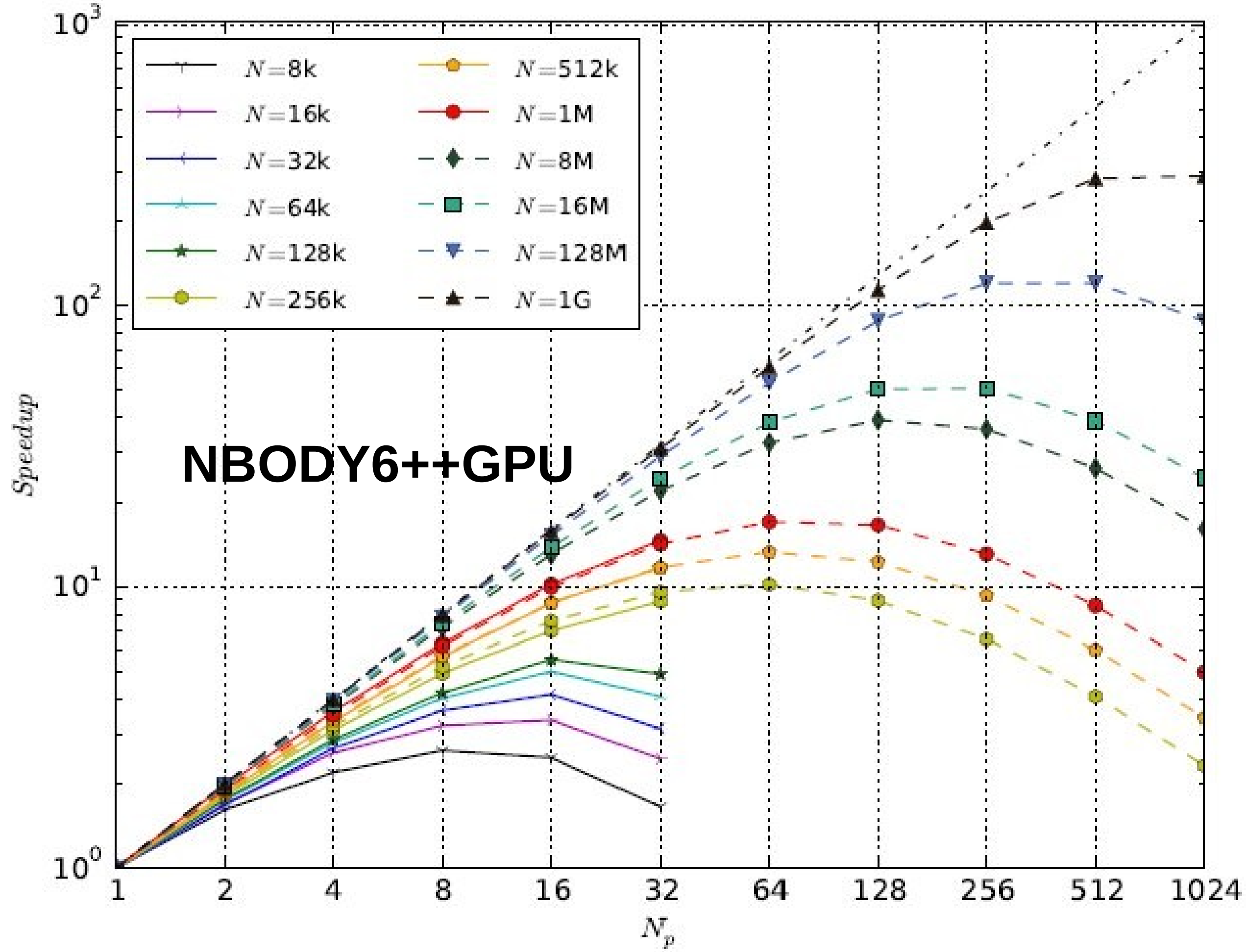

Huang, Berczik, Spurzem, Res. Astron. Astroph. 2016, 16, 11.

Fig. 2 The speed-up (S) of NBODY6++ as a function of particle number (N) and processor number (N_p). Solid points are the measured speed-up ratio between sequential and parallel wall-clock time, dash lines predict the performance of larger scale simulations further. The symbols used in figure have the magnitudes: $1k = 1,024$, $1M = 1k^2$ and $1G = 1k^3$.

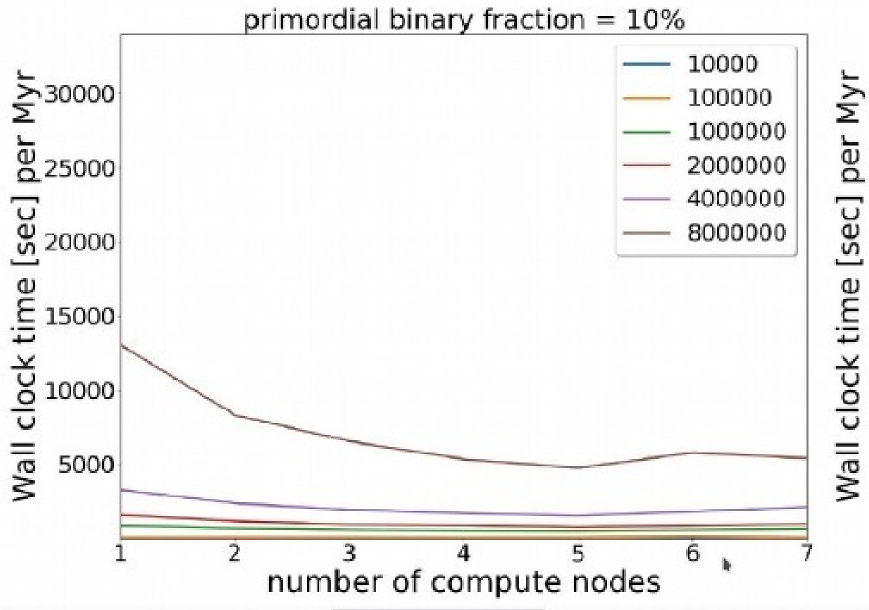

Figure 3: Scaling of PeTaR with number of nodes, 10k to 8m particles, 10% binary fraction.

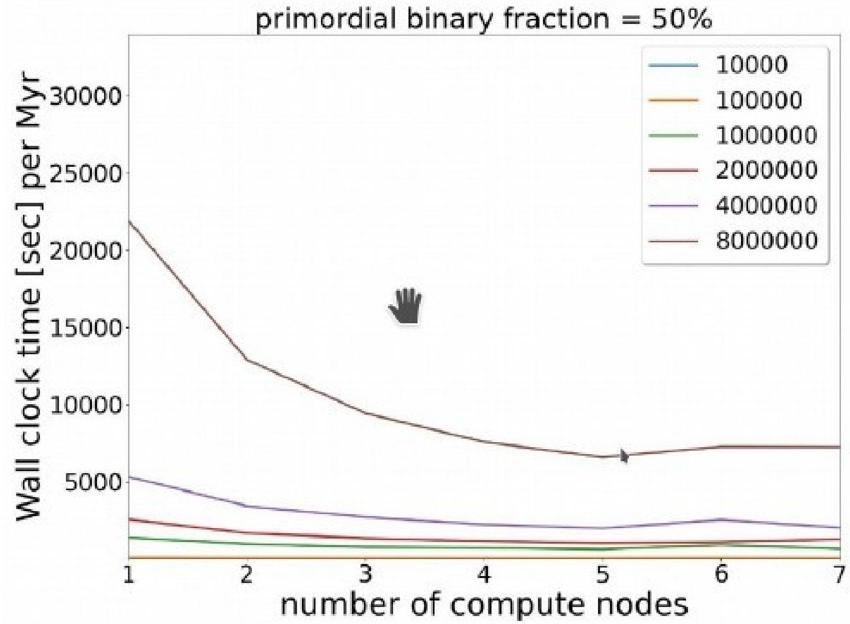

Figure 4: Scaling of PeTaR with number of nodes, 10k to 8m particles, 50% binary fraction.

From Shu Qi (Ph.D. Peking Uni 2021):
Benchmarks with PeTaR on Juwels Booster in Jülich
Up tp 8 million particles; 50% binaries
(unpublished, computing time application)

NBODY6++GPU: in progress….

北京大學
PEKING UNIVERSITY

Past, current, and future simulations with Nbody6++GPU and MOCCA

- DRAGON-I simulations of globular clusters (GC) (Wang et al. 2015, 2016, Shu et al. 2021)
- MOCCA Survey Database I of 2000 GC models (Askar et al. 2017, Morawski et al. 2018)
- Nuclear star cluster harbouring a central accreting SMBH (Panamarev et al. 2019)
- IMBH growth studies (Giersz et al. 2015, Arca Sedda et al. 2019, di Carlo et al. 2020, Rizzuto et al. 2021. Arca Sedda et al. 2021, Rizzuto et al. 2022 new s.ev.)

Issues to deal with now/next:

- Stellar evolution update (cf. other work, e.g. CMC/COSMIC (Breivik et al. 2020), MSE (Hamers et al. 2020), MOBSE2 (Giacobbo et al. 2018),….) our work: → Banerjee et al. 2020, Kamlah et al. 2021
- Relativistic kicks after PN merger (Morawski et al. 2018 and earlier); our work → Arca Sedda et al. 2021, in progress with Banerjee
- Tidal fields: (see Meiron, Webb, Hong, Spurzem, Berczik, Carlberg 2021); options 3D time-dep. field or TT 3D tidal tensor Renaud;

Current / future simulations with updated SSE/BSE:

- New MOCCA Survey Database II (chuck; Giersz, Hypki, Leveque et al.)
- DRAGON-II IMBH studies (JUWELS, binAC; Arca Sedda et al.) (incl. rotation)
- DRAGON-II of NGC 3201 (JUWELS; Kamlah, Spurzem et al.) (incl. Rotation)
- 47 Tuc, ω Cen, nuclear star clusters

Original Slide by A. Kamlah